Geomorphology 462 (2024) 109343

Contents lists available at ScienceDirect

Geomorphology

journal homepage: www.journals.elsevier.com/geomorphology

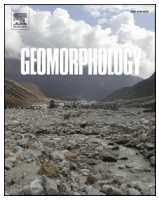

Sediment export from an Alpine proglacial area under a changing climate: Budgets, rates, and geomorphological processes

Sara Savi [a,e,*], Felix Pitscheider [b], Michael Engel [c], Velio Coviello [b,d,1], Manfred R. Strecker [e], Francesco Comiti [f]

[a] University of Pavia, Department of Earth and Environmental Sciences, via Ferrata 1, 27100 Pavia, Italy
[b] Free University of Bozen-Bolzano, Faculty of Agricultural, Environmental and Food Sciences, piazza Università, 5, 39100 Bozen-Bolzano, Italy
[c] Federal Institute of Hydrology (BfG), Am Mainzer Tor 1, 56068 Koblenz, Germany
[d] National Research Council, Research Institute for Hydrogeological Protection, Corso Stati Uniti, 4, 35127 Padova, Italy
[e] University of Potsdam, Institute of Geosciences, Karl-Liebknecht-Straße 24-25, 14476 Potsdam-Golm, Germany
[f] University of Padova, Department of Land, Environment, Agriculture and Forestry, Viale dell'Università 16, 35020 Legnaro, PD, Italy

ARTICLE INFO

Keywords:
Moraines
Proglacial streams
Glacial export
Lateral erosion
Bedload measurements
DoD measurements

ABSTRACT

Proglacial areas in the European Alps and other high-elevation mountains are currently undergoing rapid change due to global warming. Because of rising temperatures, glaciers and glacier forefields are subjected to increased melting and associated sediment export. This observation is increasingly important with respect to high-elevation geomorphological and ecological dynamics, emerging natural hazards and mitigation efforts, and hydropower plant management. It is therefore crucial to analyze the factors and feedback mechanisms governing sediment production, transport, and deposition in these rapidly changing areas.

In this study, we investigated the sediment dynamics of a proglacial area located in the Eastern Italian Alps over the period 1969–2021 with the aims of: i) identifying the areas of sediment production; ii) quantifying volumes and rates of bedload sediment transport; and iii) determining the relative contribution of glacial export and fluvial erosion to the total sediment budget. We found that i) apart from glaciers, moraines and fluvial channels have been the most important sediment sources, albeit with substantial differences in terms of connectivity and thus supply rates; ii) the volumes and rates of sediment erosion varied by one order of magnitude (between tens and hundreds of mm per year), and were generally higher along the channel network; and iii) for a relatively shorter time interval between 2005 and 2021, the relative contribution of glacial bedload input with respect to the total sediment budget ranged between 34 % and 37 %, whereas 45 % to 59 % was derived from lateral fluvial erosion. Only a relatively small sediment volume was generated by net channel bed incision. These results imply that most of the sediment released from the proglacial area of the Sulden glacier is progressively transferred to the downstream sector of the channel network, with volumes that range between 931 and 1017 tons yr^{-1} km^{-2}. These values are in the typical range of sediment export volumes from glaciated basins and highlight the high dynamicity of this region of the Alps. In general, our results confirm the complexity – in terms of spatial and temporal variability – of Alpine proglacial systems and highlight the need to systematically study these areas on a wide spatial and temporal scale, since the information provided by single locations or individual sectors of the sediment cascade, may not be adequate for understanding the dynamics acting in the entire proglacial regions.

1. Introduction

Like other high-mountain regions, proglacial areas of the European Alps are severely affected by climate warming (Gobiet et al., 2014; Hock et al., 2019; Lane et al., 2017). These regions are under increasing environmental stress with far-reaching consequences (e.g., in relation to water and sediment discharge) for adaptation and resilience policies, and with respect to downstream ecosystems, including populations

* Corresponding author at: University of Pavia, Department of Earth and Environmental Sciences, via Ferrata 1, 27100 Pavia, Italy
E-mail address: savi.sara@unipv.it (S. Savi).
[1] Deceased on April 1st, 2023.

https://doi.org/10.1016/j.geomorph.2024.109343
Received 4 December 2023; Received in revised form 4 July 2024; Accepted 11 July 2024
Available online 14 July 2024

living at low-elevation sectors (Hock et al., 2019; Zhang et al., 2022). In recent years, the impacts of climatic changes on processes in alpine proglacial areas have been frequently investigated in the context of hydrological, geomorphological, and ecological dynamics, water resources availability and management, as well as natural hazard assessments and risk mitigation policies (e.g., Carrivick and Heckmann, 2017; Huss et al., 2017; Micheletti and Lane, 2016; Savi et al., 2023, and references therein). For the preservation and the sustainable use of high-mountain environments in the coming decades (e.g., Bosson et al., 2023), it is particularly important to understand the conditions and feedback mechanisms that determine sediment production, transport and deposition in these environments.

The classical paraglacial evolutionary model (Ballantyne, 2002; Church and Ryder, 1972) suggests that during a phase of deglaciation, the sediment yield in glaciated basins initially increases due to the large volume of meltwater and unconsolidated sediment, and progressively declines until the sediment sources in the higher portions of the basin are completely depleted. However, more recent studies have shown that the complexity of natural landscapes, the nonlinearity and feedback mechanisms among hydrological processes, geomorphic conditions, and sediment transfer rarely have described a simple decline of sediment as suggested by the paraglacial model, but rather show a more complex behavior that needs to be better understood (Cossart, 2008; Knight and Harrison, 2014; Porter et al., 2019). Indeed, different runoff origins (i.e., snow and ice melt, rainfall) may activate different sediment sources depending on the season (e.g., Comiti et al., 2019), on the position of the water and sediment sources within the catchment (e.g., Carrillo and Mao, 2020), and on the intensity of the melt/rainfall event (Mao et al., 2014; Piermattei et al., 2023; Swift et al., 2002). In addition, the progressive self-adjustment of the channel network during glacier retreat may lead to the (de)coupling of new and old sediment sources along hillslopes or within the active floodplains, thereby constantly changing the connectivity between different landscape sectors (e.g., Cavalli et al., 2019; Lane et al., 2017; Micheletti and Lane, 2016). The self-reorganization of sediments within stream channels can also strongly buffer downstream sediment transfer from upstream inputs (Anderson and Konrad, 2019; Antoniazza et al., 2023; Guillon et al., 2017; Fryirs et al., 2007; Mancini et al., 2023). Finally, permafrost degradation, frost cracking, and rainfall-induced mass movements may contribute to activating new sources of sediment (e.g., Anderson and Shean, 2021; Kofler et al., 2021; McColl and Draebing, 2019; Savi et al., 2021a) and generating transient peaks of supply (Knight and Harrison, 2018; Porter et al., 2019; Slaymaker, 2009). Overall, the intrinsic spatial and temporal variability of the above processes, combined with the challenges of obtaining reliable sediment transport data in proglacial basins (Antoniazza et al., 2022; Coviello et al., 2022; Mancini et al., 2023; Mao et al., 2019; Rickenmann, 2018), limit our current understanding and make predictions of future sediment yields in glaciated river basins highly tenuous (Knight and Harrison, 2018; Porter et al., 2019).

Many recent studies have focused on the processes affecting proglacial areas from different perspectives, including the analysis of sediment sources within the basin, their connectivity within proglacial streams, and the rates of sediment transfer within the fluvial network (e.g., Comiti et al., 2019; Delaney et al., 2018; Lane et al., 2017; Mancini et al., 2023). Although these studies collectively have provided important insights into the assessment and reconstruction of sediment dynamics in alpine regions, they still leave several unanswered questions, which are the subject of this study.

In particular, these studies reveal several characteristics that appear to be common in many deglaciating basins, and that can be summarized as follows:

1. Moraines are important sources of sediment and, although they develop toward natural stabilization (e.g., Ballantyne and Benn, 1994; Curry et al., 2006; Draebing and Eichel, 2018; Eichel et al., 2018), they can remain active as sediment sources after deglaciation up to several centuries (Altmann et al., 2023; Betz-Nutz et al., 2023). The material produced along the upper (and generally steeper) part of a moraine is often deposited at its foot, thus being decoupled from the proglacial stream and floodplain (e.g., Gärtner-Roer and Bast, 2019; Mancini and Lane, 2020). Coupling may occur over decades, generally due to the erosional impact of intense rainfall events (Curry et al., 2006; Guillon et al., 2017; Savi et al., 2023).
2. Glacial transport and erosion are important sources of sediment supply, both for the material transported in suspension and as bedload (e.g., Beylich and Laute, 2015; Comiti et al., 2019; Delaney et al., 2024; Perolo et al., 2019; Schmidt et al., 2022; Swift et al., 2002). However, the relative glacial contribution to total sediment yield, especially to bedload transport, is still largely unknown (Guillon et al., 2017; Harbor and Warburton, 1993; Piermattei et al., 2023) and strongly depends on the lithology below the glacier (e.g., bedrock vs. sediment).
3. Rates of paraglacial adjustment are generally much higher than rates of fluvial erosion (e.g., Altmann et al., 2022; Curry et al., 2006), but these high rates seem to be spatially limited to proglacial areas, with little to no influence on basin-scale denudation (Antoniazza et al., 2023; Delaney et al., 2018; Koppes et al., 2010).
4. The sediment budget in the proglacial systems is extremely variable (Comiti et al., 2019; Micheletti and Lane, 2016; Savi et al., 2023) and net erosion or deposition may depend on local conditions, i.e., morphology of the channels and accommodation space (Beylich and Laute, 2015; Guillon et al., 2017; Mancini et al., 2023; Piermattei et al., 2023). As a result, many deglaciating catchments (sensu Knight and Harrison, 2018) record only relatively low rates of erosion, suggesting that most of the proglacial streams are either armored (Antoniazza et al., 2023) or disconnected from the most important sediment sources (e.g., Lane et al., 2017; Micheletti and Lane, 2016), or that the timing of sediment reorganization within the proglacial area does not allow for direct downstream propagation of the forcing (i.e., climatic) signal (Anderson and Konrad, 2019; Antoniazza et al., 2023; Mancini et al., 2023; Scorpio et al., 2022).

By building on these important insights, the main aim of our work is to understand the contribution of glaciers, moraines, and proglacial streams to the sediment budget of a proglacial plain and the overall sedimentary dynamics in the Eastern Italian Alps. In a conceptualized model, the status of a (proglacial) system – i.e., erosional, depositional or in equilibrium, can be expressed through the following equation:

$$\text{Glacial}_{SS} + \text{Paraglacial}_{SS} \approx \text{Sediment export}$$

where the glacial and paraglacial terms represent sediment input (the subscript "*SS*" stays for *sediment supply*); the term to the right of the equal sign represents the sediment reaching the outlet of the system (i.e., the outlet of the proglacial plain in this study). Paraglacial sediment supply can be interpreted as the material mobilized within the proglacial margins, including moraine slopes, proglacial streams, and the floodplain (Slaymaker, 2009). Considering the balance scale of Lane (1955), as long as water discharge can transport material supplied to the system, the proglacial system will be erosional (i.e., input $<$ export). If water discharge is insufficient to transport all material, the proglacial system will be depositional (i.e., input $>$ export). If input and export are balanced, the system is in equilibrium and the sediment dynamics are dominated by either transport (i.e., input $=$ export) or immobility (input $=$ export $= 0$).

To assess the sediment input of the proglacial area of the Sulden glacier (South Tyrol, Italy), we used a combination of tools and datasets (e.g., digital elevation models, aerial images, orthophotos, and 3D terrain analysis), which allowed us to identify the main sediment sources and to quantify the volumes and rates of net sediment erosion since 1969. Furthermore, we used the availability of continuous bedload transport data measured at the glacier terminus (Arnoldi, 2022) to

estimate the relative contribution of glacial bedload supply to the total sediment budget. With only a few exceptions (e.g., Mancini et al., 2023) this information is largely missing in similar studies. By combining this information with the quantification of the sediment mobilized within the proglacial margins, we were able to identify the status of the Sulden proglacial area, which is currently dominated by sediment transfer. Finally, by examining the morphometric characteristics of the proglacial streams and their temporal evolution, we analyzed how sediment connectivity has changed since 1969 and how it may change in the near future given the evolving climate change conditions.

2. The study area in the upper Sulden river basin

Our study focused on the proglacial area of the Sulden glacier, a large debris-covered glacier located in the Ortles/Cevedale group in South Tirol (Fig. 1), within the Sulden river basin (the basin area is about 130 km^2, max and min elevation are about 3900 m and 1100 m a.s.l., respectively). The lithologic units in the area comprise limestones and dolomitic rocks of the Ortles nappe to the west, and metamorphic rocks of the Campo nappe to the east (ISPRA, 2012). The different lithologies exert a control on the morphology of the upper basin, with the highest peaks and rock walls located in limestone units, and more gentle slopes corresponding to metamorphic bedrock (Buter et al., 2020).

The upper Sulden catchment covers an area of circa 15 km^2; in 2021 glaciers occupied a surface area of circa 5 km^2, covering 33 % of the basin (Fig. 1). Meteorological data are available from a weather station located at 2825 m (Madritsch station). Long-term (1981–2010) averaged climatic conditions define a mean annual air temperature of −2.4 °C and a mean annual precipitation of 980 mm (3PClim database). High-resolution climatic trends from the Madritsch station reveal that temperature has been increasing since the 1980s, with a deviation during the last decade (2011−2020) that on average reached +2.6 °C compared to the standard reference period (e.g., 196–1991) (Crespi et al., 2020, 2021; Savi et al., 2021a). In contrast, precipitation measurements do not show any particular trend, although a general increase in spring and summer amounts is notable (Savi et al., 2021a).

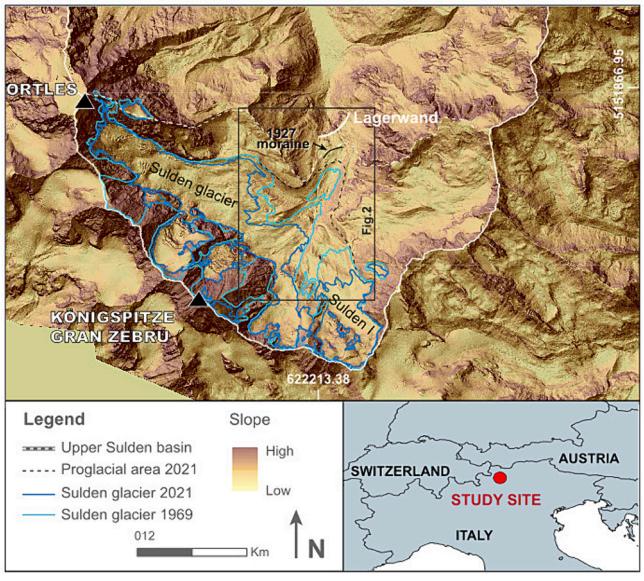

Fig. 1. Present-day extent of the Sulden glacier in the Southern Alps; white dashed line represents the upper Sulden basin; the black dashed line marks the proglacial area studied in this study. Blue lines denote former ice extents in 1969 and 2021. The gray rectangle shows the area highlighted in Fig. 2. The study site is marked by a red circle in the regional location map. (For interpretation of the references to colour in this figure legend, the reader is referred to the web version of this article.)

Considering that the number of rainfall events has not changed over time, these higher values may be associated with increasing rainfall intensity (Savi et al., 2023). Summer snow- and ice-melt events largely contribute to the runoff of the entire Sulden catchment, which is nivo-glacially dominated (Engel et al., 2018), as well as to the associated peak in bedload export (Coviello et al., 2022).

The Sulden glacier has a complex history of fluctuations, documented by numerous historical sources (e.g., Finsterwalder and Legally, 1913; von Sonklar, 1857). Savi et al. (2021b) provided a detailed reconstruction of the most important changes in glacier behavior after the Last Glacial Maximum during the Little Ice Age (LIA). With the exception of the two surge-like events that took place in the first half of the 19th century, most of the glacial fluctuations occurred in the area within the well-exposed LIA moraines, above a bedrock step known as *Lagerwand* (Fig. 1), which is also the area investigated in this study. Here, we will use the term *proglacial area* referring to this area of the basin (which in 2021 covered ca. 1.85 km^2), which ends immediately above the terminal moraine marking the 1927 glacier advance (Fig. 1). This contrasts with the use of the term *proglacial area*, as defined by Carrivick and Heckmann (2017) as the area limited by the LIA terminal moraine. We made this choice to avoid an area where human activity (i.e., road construction and water intake infrastructures) has modified the morphology of the glacial landscape, and because the LIA terminal moraine is no longer visible in the landscape (Savi et al., 2021b).

In 1945, the glacier comprised a single ice body with a prominent tongue that flowed north, occupying the main valley (Savi et al., 2021b; Fig. 2). Today, glacier retreat has exposed large amounts of unconsolidated sediment. Interestingly, a large portion of the Sulden glacier appears to flow on a 40 to 60-cm-thick consolidated layer of conglomeratic sediment that remains largely unaffected by the glacier passage and forms a plateau (Fig. S1 of the supplementary material). Over this consolidated layer, moraines from past phases of glacial advance as well as drumlin-like features are preserved in the topography and help documenting the dynamics of the glacier over time. A similar layer also exists at the base of the central front of the Sulden glacier (Fig. S2), where the proglacial stream has partially cut into it, eroding the less consolidated sediment below.

In 2021 (Fig. 1 and Fig. 2), the Sulden glacier featured two main outflow channels, one exiting on the western side of the glacier and one on its central part (referred to as Western Sulden and Central Sulden, respectively, in Savi et al., 2021b). The western channel flows on a bed of coarse sediment within a fairly narrow area (20 m wide on average) that skims the LIA lateral moraine and the middle moraine. In its upper section, the channel bed has an average slope of ca. 13°, which decreases to 8.5°after merging with the stream coming from the central sector. The stream originates from the main Sulden glacier terminus and flows on a small braid plain. After ca. 100 m, the stream receives runoff from the Sulden I glacier (Fig. 1) before flowing through a narrow bedrock gorge and reaching the confluence with the western outflow channel. Below this confluence, a wide braid plain, confined by the lateral LIA moraines, extends downstream until the terminal moraine of the 1927 glacier advance (Savi et al., 2021b; Fig. 2).

Over the past 30 years, the growing amount of debris covering the glacier surface at higher altitudes (Savi et al., 2021b) reflects the increased instability of the surrounding slopes (Savi et al., 2021a) and contributes to the volume of material that can be incorporated into the ice and lateral moraines (Rabanser, 2019). Previous studies demonstrated that these sediments, in combination with debris from the receding glacier, are an important source of sediment for the proglacial plain and exert a decisive control on both the reorganization of the drainage network and sediment connectivity (Buter et al., 2022; Savi et al., 2023). Bedload and suspended sediment are also an important source of clastic input to the total sediment flux, albeit with large daily and seasonal differences that are likely controlled by subglacial meltwater dynamics and temperature variations (Arnoldi, 2022; Coviello et al., 2022; Engel et al., 2020, 2024).

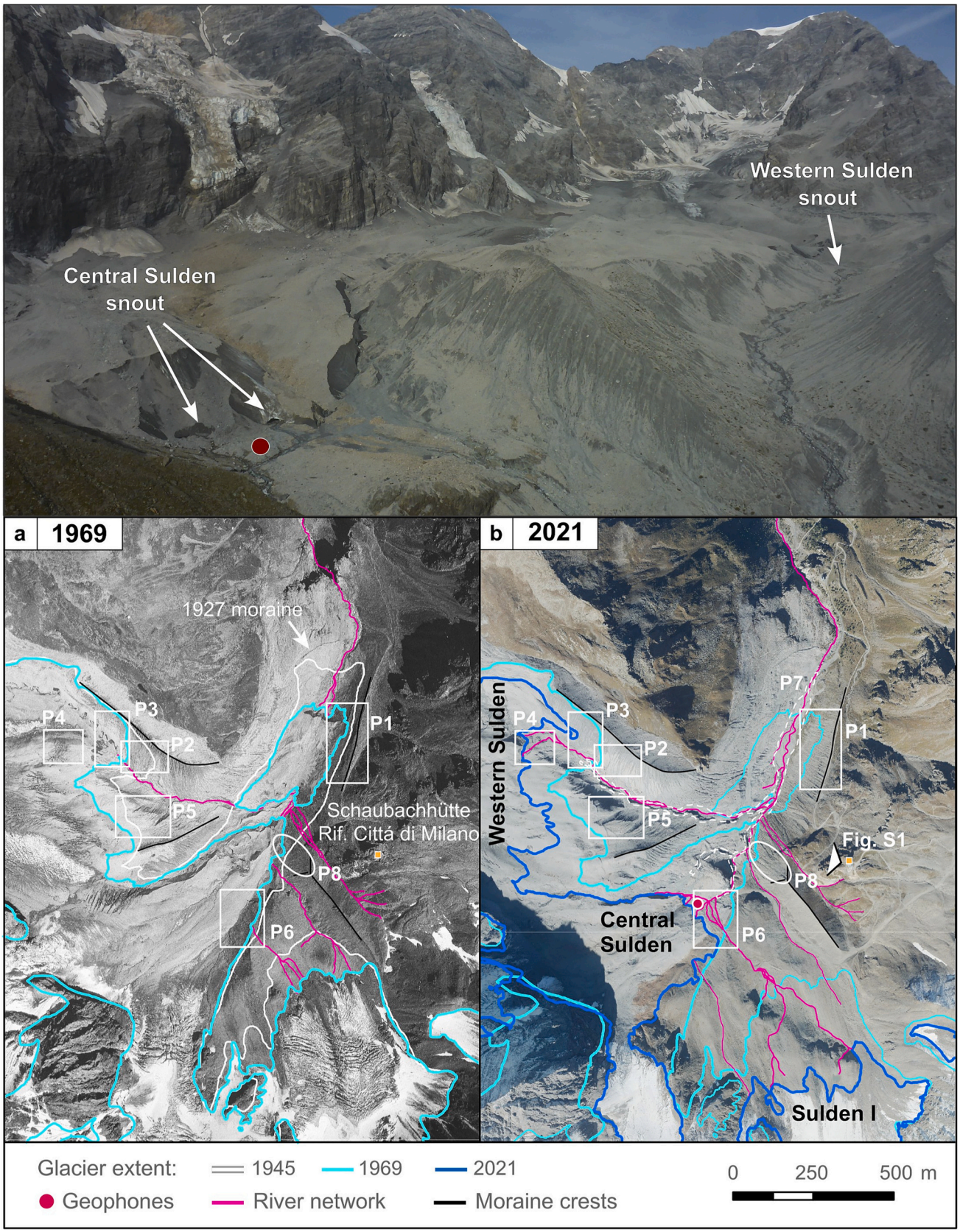

Fig. 2. Upper panel: a photograph of the Sulden glacier in 2020 with the indication of the central and western outflows. Lower panels: The proglacial area of the Sulden glacier with the locations of the eight areas analyzed in the study and the differences visible between a) 1969 and b) 2021. White dashed line in panel b) represents the area analyzed along the channel network.

3. Materials and methods

3.1. Aerial images, orthophotos, and digital surface models

To reconstruct the evolution of the proglacial area of the Sulden glacier we used different tools and resources available for the study region (see also the supplementary material). In particular, we used different sets of aerial photographs and orthophotos starting from 1945 (Table 1). The 1969 aerial image, which has by far the highest resolution of all aerial photos (collected at a scale of 1:21.000), was used to evaluate changes along the moraines, and calculate volumes and rates of sediment mobilization. This image was compared to the orthophotos acquired in 2005 and 2021, in combination with ALS (Aerial Laser Scanning). These LiDAR-based surveys were used to extract high-resolution (e.g., 1 m) digital surface models (DSMs), and to create a DEM of Difference (DoD) used to quantify topographic changes over the moraines and within the proglacial area.

Additional aerial/ortho photos (e.g., taken in 2013, 2016, 2017, 2018, 2019, and 2020) and LiDAR-derived DSMs, with corresponding DoDs (e.g., generated for the periods 2013–2021, 2018–2021, and 2019–2021), were used in a few locations to better understand the reorganization of the drainage network that followed glacier retreat. This data provided important information on the dynamics and timing related to the activation of different sediment sources.

All DSMs were created from LiDAR-derived point clouds using the Cloud Compare software (https://www.cloudcompare.org/). To minimize systematic errors, the different point clouds were first aligned with the ICP (i.e., *Iterative Closest Point*) method (Besl and McKay, 1992) with respect to the 2018 point cloud, i.e., the data set with the highest quality. Subsequently, differences between two surveys (i.e., changes) were identified with the *cloud-to-cloud* comparison tool (Lague et al., 2013; Nourbakhshbeidokhti et al., 2019). The resulting DoD point clouds were extracted as raster (1 m resolution) for further analysis using the ArcGIS software. Considering that the different point clouds had different point densities, the precision with which the alignment could be done, differed for the different datasets. As such, the different DoDs had also different errors. For the longest time period (2005–2021), the mean error derived from DEMs alignments was 0.1 m. For the shorter time periods (2018–2021, and 2019–2021) mean errors were approximately 0.05 m.

For the DoD analysis, which were carried out in accordance with previous studies based on ALS-derived elevation models, we adopted a threshold value (or minimum Level of Detection –- LOD) to exclude small elevation changes that are not statistically significant to be considered as real with respect to the individual DoD precision (Wheaton et al., 2010; Cavalli et al., 2013; Savi et al., 2023). The threshold was selected with caution to be ±0.2 m, based on the propagated vertical and horizontal uncertainties reported by the company contracted for the ALS flight, which were verified by several point checks on stable surfaces within the surveyed area (refuge roof, ski slope, parking lot). Therefore, in the net volumes calculated from the DoD analysis, the error was calculated by multiplying the threshold value by the area of the observed topographic change, whereas for total budgets we used standard theory of error propagation (i.e., Taylor, 1997; Wheaton et al., 2010).

3.2. Delineation of the different morphologies

The glacier extent in different time periods was obtained in different ways. For the 1945 and 1969 time periods, the glacial extent was manually delineated based on the details visible on the aerial images. These limits are the least accurate, because in some areas, especially along the debris-covered area of the glacier, the real ice extent was not easily distinguishable from other debris. For the years 2005 and 2017, we used the official, open-access glacier distribution published by the Bozen/Bolzano Province on their Geocatalog website. These glacial extents were obtained with different tools, including DoD analyses, and mark the extent of both glacier and ground ice incorporated into the lateral moraines. For 2018, 2019, and 2021, the glacier extent was obtained through DoD analyses and visual inspection using orthophotos. These limits refer to the glacier extent only, and do not include ground ice. Ground ice delineation is possible only through DoD analysis, since it does not leave morphological evidence at surface, but it is generally associated with a small reduction in topography that can be detected by DoD analysis. Conversely, glacier melt is associated with a profound modification of the surface, as the glacier morphology vanishes during glacier retreat. As such, the difference between the two types of ice melt is well distinguishable, whereas it is more difficult to separate ground ice melting from erosion occurring on the moraines due to the small volumes that both processes generate.

The delineation of the proglacial plain was based on the inspection of orthophotos and on the slope maps derived from the DEMs. We distinguished between *active channels*, limited to the narrowest and most incised areas where the proglacial streams are flowing and are able to laterally move, from the *proglacial channel network*, defined as the entire channel network, thus also including riverbanks (Fig. S1 of the supplementary material).

3.3. Sediment export: volumes, rates, connectivity and channel profiles

In total, we analyzed the topographic changes at six locations (hereafter called P1 to P6) within the study area (Fig. 2), with the addition of the changes along the channel network (P7) and of those caused by a large landslide that occurred on the eastern LIA moraine in 2014 (P8) (Savi et al., 2023; Steger et al., 2022). Among the six areas analyzed at the margin of the glacier, three are located on the LIA moraines (P1, P2 and P3 in Fig. 2) and three are along the modern and paleo-drainage network in the proglacial plain (P4, P5 and P6 in Fig. 2). Three locations (P1, P2, and P5) allowed detecting changes that have occurred since 1969 (Table 2), because these areas were already ice-free

Table 1
Available data for the study area (*from* Italian Military Geography Institute[1]; Province of Bozen/Bolzano[2]; Free University of Bozen/Bolzano[3]; University of Potsdam[4]).

Period	Type of data	Scale/Resolution
1945[2], 1954[2], 1959[1], 1969[1], 1989[2]	Aerial Photographs	Scale from 1:63.000 (1945) to 1:21.000 (1969)
1982–85[2], 1992–96[2], 1999[2], 2000[2], 2003[2], 2006[2], 2008[2], 2011[2], 2016[2], 2018[3], 2019[3], 2020[2], 2021[3,4]	Orthophotos	From 1.0 m (old ones) to 0.20 m (new ones)
2013, 2017, 2021	ENSRI/Google Maps photos	unknown
2005[2], 2013[3], 2016[2], 2018[3], 2019[3], 2021[3,4]	Point Clouds/ DEMs	From to 2.7 pt./m^2 (2013) to 8.2 pt./m2 (2018)

Table 2
Summary of the studied areas with associated time periods and method used for the quantification of the eroded volumes.

Location	Analyzed time periods	Method
P1 (East moraine)	1969–2021; 2005–2021	Topographic reconstruction; DoD
P2 (West moraine)	1969–2021; 2005–2021	Topographic reconstruction; DoD
P3 (West moraine)	2019–2021	DoD
P4 (Modern drainage network)	2013–2021	DoD
P5 (Paleo drainage network - Middle moraine)	1969–2021	Topographic reconstruction
P6 (Modern drainage network)	2013–2021	DoD
P7 (Channel network)	2005–2021	DoD
P8 (Landlside)	2013–2021	DoD

at that time. In contrast, locations P3, P4 and P6 were ice-covered until recently (i.e., 2005 or later), and were analyzed over shorter timescales depending on the timing of deglaciation (Table 2). In particular, point P3 shows the changes that occurred at the margin of the glacier only between 2019 and 2021 and was added to the study to highlight some geomorphic similarities (i.e., break-in-slope morphology and delays in gully development) that we can observe also in the older, more modified landscape as recorded on the aerial images from 1969. The changes along the channel network (P7) were analyzed over the 2005–2021 time period, as this is the longest timespan we can cover with our DoD. As such, the analyzed area does not consider the most recent deglaciated area of the proglacial plain, which was below glacial ice until 2005 (Fig. 2).

To calculate the changes that occurred over the longest time period (i.e., 1969–2021), we reconstructed the paleo-topography of the most pronounced erosional features by using the 2021 DSM and the *topo2raster* function implemented in the ArcGIS software (ESRI). To achieve this, we first generated 2 m isolines from the 2021 DSM, then carved the outline of the areas of interest by cutting the isolines at the boundary of the eroded feature that we wanted to analyze. We finally reconstructed the paleo-topography with the *topo2raster* function that, starting from the existing isolines, interpolates elevation data in the areas without information, thereby reconstructing the most probable paleo-surface of the eroded feature (Szypuła, 2019; more details in Fig. S3 of the supplementary file). Volumetric changes were calculated by subtracting the reconstructed paleo-surface from the 2021 DSM. Associated errors were determined by averaging elevation changes in stable areas (e.g., outside of the eroded feature where surfaces have not changed) and by multiplying this value for the area of interest (Lane et al., 2003).

In addition to the volume calculations, rates of topographic variations were retrieved by dividing the total volume by the analyzed area and by the number of years covered by the analyses. For example, an eroded volume of 500 m^3 over an area of 20,000 m^2 between 2005 and 2021 (i.e., 16 years), would result in an erosion rate of 1.56 mm yr^{-1}. This was done to have a metrics that can be more easily compared to the data obtained in other studies, where detailed information on the extent of the analyzed areas is not always reported.

By looking at the variations between the 2005 and 2021 DSMs, we additionally analyzed changes in sediment connectivity within the proglacial plain by applying the method proposed by Cavalli et al. (2013) after resampling the available DEMs to a 2.5 m resolution; this method uses a DEM to calculate slope and contributing areas for every pixel on the surface. By computing a weighted product between these two variables, the method defines a connectivity index that highlights areas most connected to the drainage network, relative to either the entire fluvial system or the outlet of the catchment (Borselli et al., 2008; Cavalli et al., 2013). Variations in the channel network were further investigated in terms of changes along longitudinal profiles and cross sections. In particular, we analyzed channel width variations by mapping the topographic changes along the active channel bed. To do this, we manually delineated the active channels on the 2005 and 2018 orthophotos as explained above, and quantified the relative contribution of fluvial lateral erosion to the total amount of sediment calculated through our DoD analyses.

3.4. Bedload export from the glacier terminus

Continuous estimations of bedload fluxes and total volumes are available for the summers of 2019 and 2020 for the area located at the main Sulden glacier terminus (Arnoldi, 2022). Three seismic sensors (vertical geophones with a natural frequency of 4.5 Hz) connected to a portable acquisition station ("Datacube" manufactured by the "Digos" company) were installed in the proximity of the glacier snout (Fig. 2), on the proglacial braid-plain, from the beginning of July to the end of August. The acquired seismic signal (i.e., amplitude) was calibrated through 35 direct bedload measurements made by using the same approach adopted in Dell'Agnese et al. (2014); Carrillo and Mao (2020), and Coviello et al. (2022), producing continuous bedload data (kg/min) over the surveyed seasons. More details on the technique and data calibration are outlined in Coviello et al. (2022), whereas measurements and related uncertainties are described in Arnoldi (2022). Because bedload yield estimations at the glacier terminus were computed in mass units (kg) and volumes obtained from our DoD analyses were computed in m^3, we converted bedload mass to bulk volume by using a mean density of 1700 kg/m^3 including porosity (as in Delaney et al., 2018, and Hinderer et al., 2013). Due to the vicinity of the three seismic sensors to the main glacier snout at an average distance of <80 m, it is important to highlight that under normal climatic conditions (without thunderstorms the bedload measurements can be considered to represent transport derived from subglacial conduits, with only a minor fraction indicative of fluvial transport. As such, in this study we used the bedload measurements at the glacier snout to attempt a first-order estimate of the glacial contribution to the total sediment budget contributed by glacial and fluvial transport, and calculated for the entire proglacial plain by DoD analysis. Total bedload transport at the glacier terminus was estimated to be about 1.7 10^7 kg (ca. 10,100 m^3) and 1.1 10^6 kg (ca. 650 m^3) for the 2019 and 2020 summers, respectively (Arnoldi, 2022). However, almost 80 % of the bedload measured in 2019 was transported during a single flood event that scoured a large portion of the proglacial floodplain immediately at the front of the glacier terminus. By removing this storm-driven bedload volume, the total bedload transport at the glacier terminus in 2019 – mostly associated with melt flows – resulted to be about 2100 m^3. Considering that the ALS flights of 2018 and 2021 were conducted in September, and that bedload transport in the Sulden proglacial area mostly occurs in summer (from June to September, based on repeated observations by the authors), the 2018–2021 DoD of the proglacial area represents the net topographic change due to the cumulative sediment fluxes that occurred during the summers of 2019, 2020, and 2021. Therefore, in order to integrate field-based bedload estimations with DoD results, we had to assume a total bedload transport value for the summer of 2021. In absence of better alternatives and data, and because no pronounced rainstorms occurred in the upper basin during the summer of 2021, we estimated the 2021 bedload yield – at least in terms of order of magnitude – as the arithmetic average of bedload yields of 2019 and 2020 (equal to 1375 m^3), calculated excluding the bedload transport volumes associated to intense rainstorm events. Limitation of this approach will be discussed later in Section 5.5.

4. Results

4.1. Proglacial plain development (1945–2021)

From 1945 to 2021, the Sulden glacier lost an area of approximately 2.71 km^2. Of this, 0.86 km^2, or 32 % of the total area, was lost in only 16 years, starting from 2005. At the same time, the proglacial area of the Sulden glacier increased by about 1.15 km^2, of which 0.74 km^2 or approximately 65 % has been gained since 2005. The difference between these two areas is due to the portion of the glacier that disappeared at high elevations (i.e., along ridges or in proximity to bedrock cliffs) and not at the glacier front.

By 2005, the glacier terminus had retreated by approximately 1 km compared to 1945, and the newly developed drainage pattern in the proglacial area (including the new stream network draining the recently deglaciated terrain) had gained around 4.7 km of channels (i.e., an average of ca. 78 m per year). By 2021, the glacier had further retreated by ca. 330 m, and 1.2 km of channels had been added to the drainage network of the proglacial plain, with an increase of 26 % at a rate of about 75 m per year.

4.2. Topographic changes, budgets, and rates

4.2.1. Eastern LIA moraine – P1

Fig. 3 illustrates the topographic changes that occurred in the lower proglacial area between 1969 and 2021 (P1). Besides the large portion of dead ice visible in the 1969 photo, other changes on the eastern LIA moraine are evident (Fig. 3). The aerial images show the development of a gully system where three distinct areas can be distinguished: i) large and deep gullies formed on the upper part of the moraine, generally above the limit of the glacier in 1969; ii) a more homogeneous slope dominating the middle part of the moraine; and iii) sediment deposits accumulated at the toe of the moraine. The presence of stable vegetation at the base of the moraine, especially in the northern section, indicates the decoupling between the moraine and the fluvial processes acting on the proglacial plain. In addition, a comparison of the position of the moraine crest relative to two large, stable boulders on the eastern side of the moraine (arrows in Fig. 3) points to a significant (10 m on average) upward migration of the gully heads (i.e., headward erosion). Furthermore, aerial images from 1969 show a break-in-slope on the eastern moraine slope, corresponding to the former upper limit of the glacier in 1954. This line represents the accumulation of material at the top of the glacier and is similar to the deposits visible on top of the dead ice block. Erosion of this latter feature was not rapid, as it was still visible in the 1985 orthophoto. Finally, another interesting observation regards the area where the moraine is today most dissected by the gully system, as it corresponds to its steeper portion above the 1945 glacier limit.

For the P1 area, the eroded volume of the gully system (i.e., the upper part of the moraine) calculated with the topographic reconstruction for the period between 1969 and 2021 yielded a value of 29,800 ± 11,020 m^3, corresponding to an erosion rate of 18.8 ± 6.9 mm yr^{-1}. Over the same area, the eroded volume between 2005 and 2021, and calculated by DoD analysis, amounts to 9340 ± 2920 m^3, which equals an erosion rate of 19.1 ± 6.0 mm yr^{-1}.

4.2.2. Western LIA moraine – P2

Moving now to the western LIA moraine (P2 area in Fig. 2), Fig. 4 shows the changes between 1969 and 2021. In 1969, the upper part of the moraine already had a fairly well-developed gully system, and by 2021 the gullies had further widened and erosion had propagated both upward (headward erosion, violet lines in Fig. 4) and downslope on the moraine through incision (between the pink lines in Fig. 4). At the moraine base, small fans had developed over time, and their presence points to a decoupling between the moraine dynamics and the fluvial channel flowing in the proximity of its toe, similar to what was observed on the eastern LIA moraine.

Because it was not possible to quantify sediment erosion on the upper moraine before 1969 – due to the unavailability of earlier aerial photos of sufficiently high resolution – we focused on the sediment export from the middle section of the moraine (delimited by the pink lines in Fig. 4), where erosional forms were not visible in the 1969 aerial photo. For this area, a minimum eroded volume of 10,190 ± 3990 m^3 was calculated from 1969 to 2021, corresponding to a minimum erosion rate of 6.8 ± 2.7 mm yr^{-1}. For the same area, the 2005–2021 DoD analysis indicated an eroded volume of 920 ± 365 m^3 and a deposited volume of 1290 ± 710 m^3. Over the entire slope (excluding the area that showed evidence of ground ice in 2005), the eroded volume on the 2005–2021 DoD was 3060 ± 1130 m^3, whereas the deposited volume was 4750 ± 2190 m^3, corresponding to a mean erosion rate of 11.5 ± 4.2 mm yr^{-1}. Our DoD analysis also indicates that ground-ice melting occurred over the entire moraine slope that was exposed by glacier retreat after 1985 (Fig. 5).

4.2.3. Western LIA moraine – P3

Fig. 5 shows the 2019–2021 topographic changes on the western LIA moraine in the section closest to the glacier terminus (P3). On the 2019 DSM, it is possible to see how the middle portion of the moraine presents a relatively smooth topography, with a developed gully system visible only in the upper moraine section (i.e., above the limit of the 2005 glacier extent, Fig. 5). In 2019, the break-in-slope marking the former

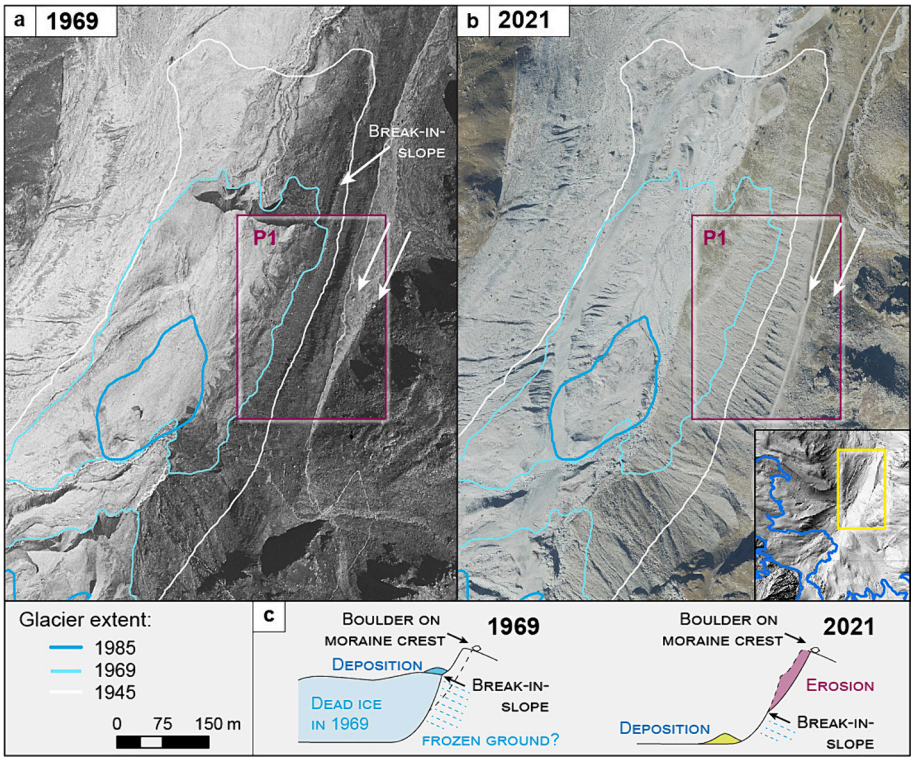

Fig. 3. Location of P1 (purple rectangle) on the eastern LIA moraine in a) 1969 and b) 2021; c) sketch of the moraine evolution between 1969 and 2021. Note that the white arrows inside the rectangle point to two large boulders that help estimating the degree of erosion along the moraine crest. (For interpretation of the references to colour in this figure legend, the reader is referred to the web version of this article.)

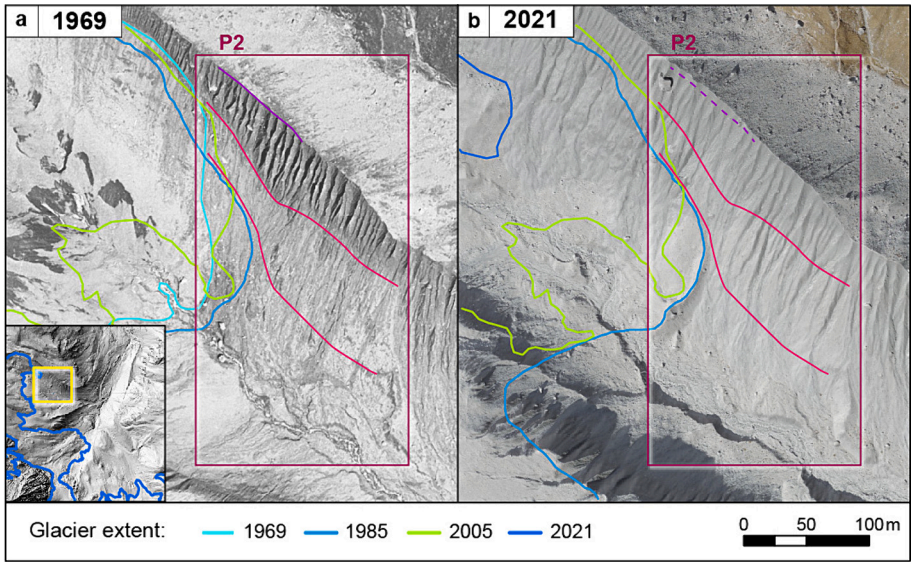

Fig. 4. Location of P2 (purple rectangle) on the western LIA moraine in a) 1969 and b) 2021. Dashed violet line indicates the retrogressive erosion along the moraine crest. Pink continuous lines indicate the area where gullies developed more between 1969 and 2021. (For interpretation of the references to colour in this figure legend, the reader is referred to the web version of this article.)

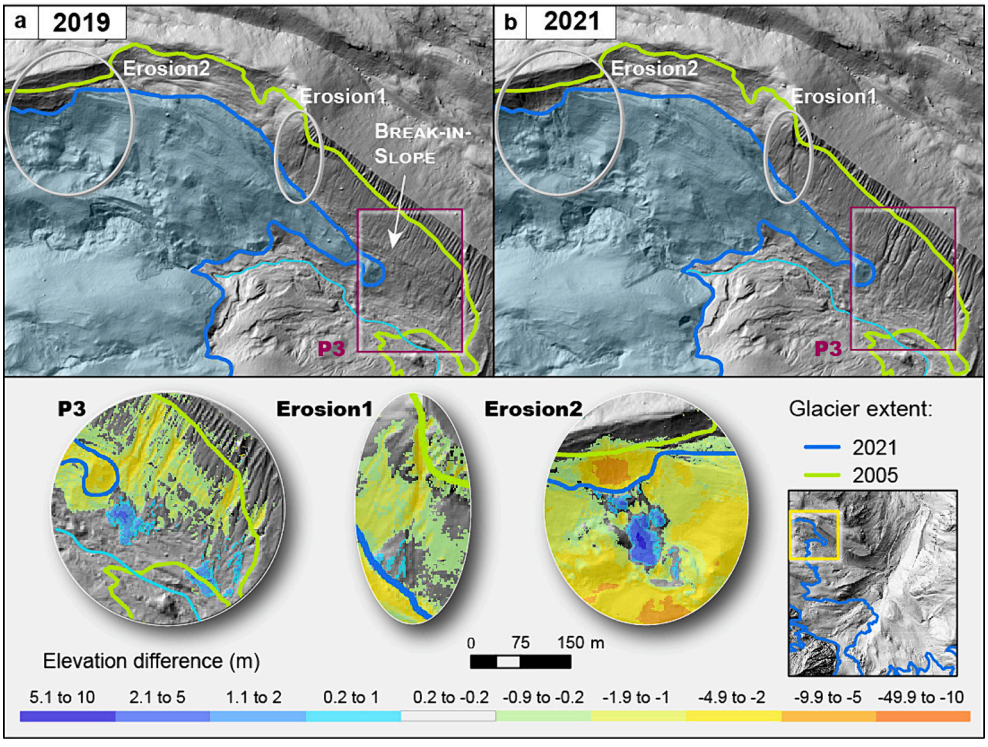

Fig. 5. Location of P3 (purple rectangle) on the western LIA moraine in a) 2019 and b) 2021. In the lower panel, the elevation difference between 2019 and 2021 in three locations highlighted in the fig. (P3, Erosion1 and Erosion2, see text). (For interpretation of the references to colour in this figure legend, the reader is referred to the web version of this article.)

position of the glacier is also visible (Fig. 5a, P3). Instead, for the year 2021, the moraine slope displays deeply incised channels that developed downslope from gully heads (Fig. 5b, P3), erasing the former topographic signature. The 2019–2021 DoD indicates an eroded volume of 6530 ± 2095 m^3 and a deposited volume of 2060 ± 610 m^3, suggesting that >4000 m^3 of material was entrained into the proglacial stream.

Fig. 5 also illustrates the influence of other erosional processes, particularly gully erosion with the formation of a fan (Fig. 5, Erosion1) and the removal of material by mass movements (Fig. 5, Erosion2) observed at the top margin of the glacier.

4.2.4. *Western proglacial stream – P4 and P5*

Closer to the glacier terminus, but on the right side of the proglacial stream, we analyzed the changes caused by the self-reorganization of the channel network following progressive glacier retreat (P4). This region showed the effects of highly dynamic changes with the successive formation and deactivation of different channels, each active for only 1 to 4 years (Fig. 6). The timing of channel activity (analyzed here from 2013

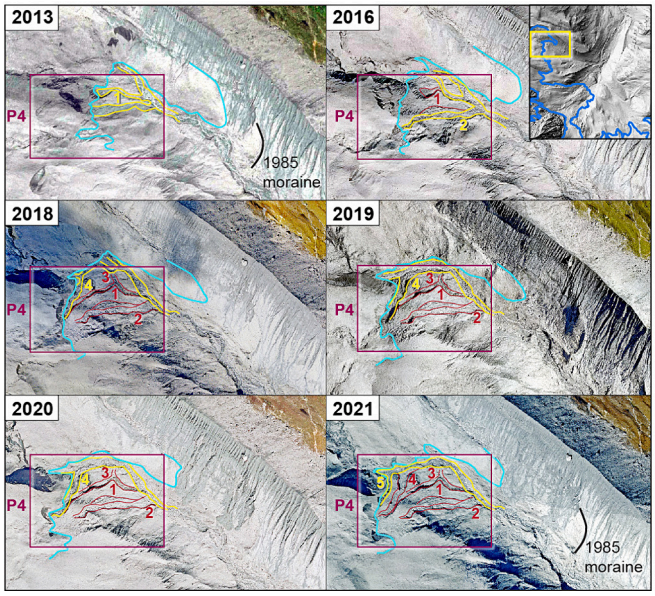

Fig. 6. Progressive development of new channels (in yellow) following glacier retreat at the terminus of the western sector of the Sulden glacier (glacier terminus highlighted for each time step in cyan; P4 in the purple rectangle). Yellow lines and numbers mark the position of the active channel in the corresponding orthophoto. Red lines and numbers indicate the isolated/abandoned channels. From 2016 to 2018, the proglacial outflow was particularly dynamic, with water (i.e., channel 2) running south of channel 1 in 2016, and water (channel 4) flowing west of channel 3 in 2018. Channel 4 widened in 2019 and 2020 but it remained in the same position until 2021, when a new channel developed farther west, isolating channel 4 and starting to form a new pathway (channel 5). (For interpretation of the references to colour in this figure legend, the reader is referred to the web version of this article.)

to 2021) reflects the speed and mechanisms of glacier retreat. This involved channels that were active for a longer time and that were associated with a stationary position of the glacier terminus; in contrast, stages with faster changes in glacier position resulted in rapid development of new channels and subsequent isolation of previous ones. The DoD analysis for this region allowed quantifying the changes that had occurred after 2013, resulting in an eroded volume of 9100 ± 1180 m^3 and a deposited volume of 650 ± 390 m^3. This indicates that 8450 ± 1245 m^3 of material was entrained into the fluvial system, with a supply rate of 62.5 ± 9.2 mm yr^{-1}.

Approximately 500 m downstream, on the right-hand side of the proglacial stream, we noticed another prominent erosional feature that began to develop from the margin of the middle moraine in 1985 (Fig. 7, P5). Here, our topographic reconstruction revealed an erosional volume of 47,560 ± 2345 m^3 and a depositional volume of 7600 ± 845 m^3, with 39,970 ± 3200 m^3 of material transferred to the proglacial stream. Analysis of the orthophotos indicated that the glacier extent in 1985 was very close to a small gully head (Fig. 7a), suggesting that during the subsequent retreat, enhanced ice melt drained into this pre-existing feature and contributed to sediment erosion. By 1996, this process was complete, as indicated by the dissection of the fan at the bottom of the proglacial channel on the corresponding orthophoto (not shown here). This extremely fast erosion occurred within a maximum time span of 10 years, providing an exceptional supply rate of 462.7 ± 37 mm yr^{-1}.

4.2.5. *Eastern proglacial stream – P6*

The evolution in area P6 is closely linked with the changes caused by the proglacial stream originating from the eastern part of the Sulden glacier (i.e., the Sulden I, Fig. 1). In 2005, this proglacial stream flowed against the eastern flank of the Sulden glacier, contributing to ice erosion, and likely continued to flow beneath the ice until it emerged again at the glacier terminus (Fig. 8).

In 2013, the Sulden glacier retreated behind the junction with the proglacial stream coming from the Sulden I and the proglacial stream exiting the main Sulden glacier. The Sulden I proglacial stream started to mobilize the material previously deposited on a small lateral moraine left by the 1985 glacier advance, redistributing sediment along the slope and onto the braid plain. As the new material is sourced from metamorphic bedrock underlying the eastern sectors of the Sulden basin, the difference between the 1985 moraine deposit, mainly composed of limestones, and the newly transported sediment is easily discernible

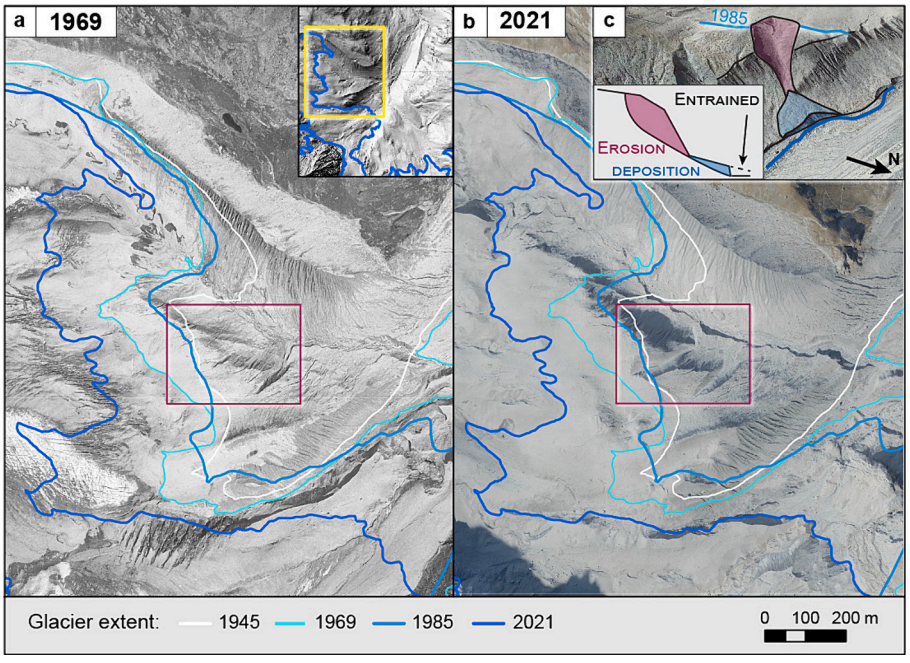

Fig. 7. Location of P5 (purple rectangle) along the border of the middle moraine in a) 1969 and b) 2021; c) depicts the process of gullying. (For interpretation of the references to colour in this figure legend, the reader is referred to the web version of this article.)

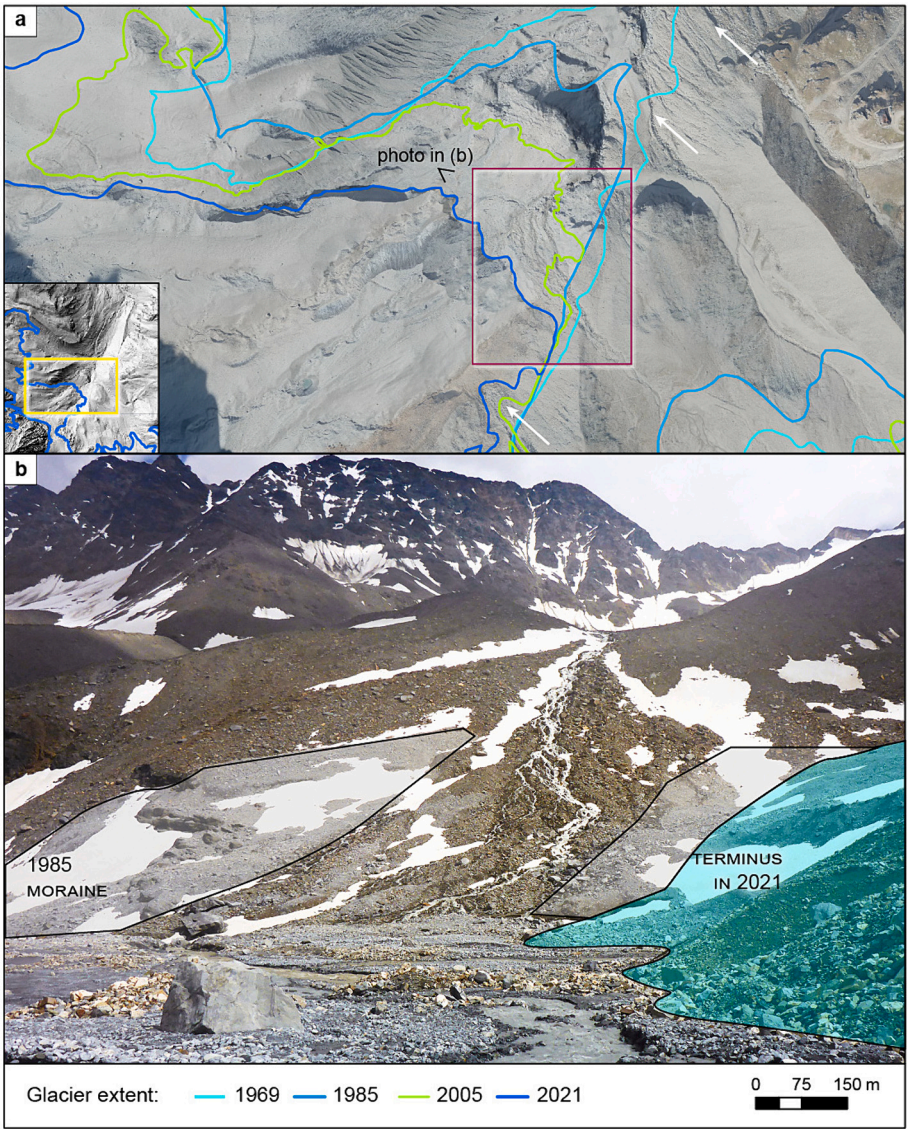

Fig. 8. a) Location of P6 (purple rectangle) and b) frontal view of the fan formed after 2013; the different colors of the material help distinguish the 1985 glacial till (in gray) from the newly mobilized material (in brown). White arrows at the glacier margin in a) indicate the locations where channels have developed in the past (to the north) and may develop in future (to the south). (For interpretation of the references to colour in this figure legend, the reader is referred to the web version of this article.)

based on the colors (Fig. 8, gray versus brown). The DoD calculations for the interval between 2013 and 2021 provides an eroded volume of 2080 ± 270 m^3 and a deposited volume of 630 ± 160 m^3, resulting in 1450 ± 315 m^3 of sediments supplied to the proglacial braid-plain (i.e., about 21.1 ± 4.6 mm yr^{-1}). This pattern of new channel development at the glacier snout and consequent sediment redistribution had occurred repeatedly in the past (Fig. 2 and Fig. 8) and will likely occur again in the future (Fig. 8).

4.2.6. *Eastern LIA moraine – landslide (P8)*

Finally, for comparison, we report the volume of sediment mobilized by a large landslide on the eastern LIA moraine that had occurred in 2014 following intense rainfalls (Savi et al., 2023; Steger et al., 2022) (Fig. 2; Table 3). During the landsliding event, a large amount of sediment (ca. 8750 m^3) was mobilized from the upper slope of the moraine, although most of it (ca. 5500 m^3) was deposited downslope on the moraine itself (Savi et al., 2023). In subsequent years, the landslide deposit continued to provide sediment; in 2021 the eroded sediment reached a total volume of 11,730 ± 1270 m^3 of eroded material and a deposited volume of 7100 ± 1570 m^3. Consequently, a volume of only 4630 ± 2020 m^3 of sediment was supplied to the proglacial stream between 2013 and 2021, at an average rate of 22.8 ± 9.9 mm yr^{-1}.

4.3. *Morphological variations along the proglacial channels and sediment transfer (P7)*

Based on the 2005–2021 and 2018–2021 DoDs, we additionally quantified the changes that had occurred in the proglacial channel network (Fig. 9).

In the period 2018–2021, the mean annual volume of sediment mobilized through the active channel network equaled 3250 ± 950 m^3 yr^{-1}. Of this, 2050 ± 750 m^3 yr^{-1} (i.e., 63 %) was eroded from the channel bed, while 1200 ± 500 m^3 yr^{-1} (37 %) was deposited, for a net sediment loss of 950 ± 950 m^3 yr^{-1}. Even if associated with a large error, mainly due to the propagating error method, this amount represents 21 % of the total volume of sediment transported to the outlet of the proglacial braid-plain, whereas 34 % (i.e., about 1375 m^3 yr^{-1}) and 45 % (i.e., about 1800 m^3 yr^{-1}) came from glacial supply (i.e.,

Table 3
Summary of the volumes and rates calculated for all analyzed areas.

Location	Method and period covered	Eroded sediment (m^3) + error	Deposited sediment (m^3) + error	Sediment supplied to proglacial stream (m^3) + error	Erosion rate (mm yr^{-1}) + error	Supply rate (mm yr^{-1}) + error
P1 (eastern LIA moraine) *active*	*Topographic reconstruction 1969–2021*	29,800 ± 11,020	–	–	18.8 ± 6.9	–
	DoD 2005–2021	9340 ± 2920	1470 ± 825	–	19.1 ± 6.0	–
P2 (western LIA moraine) *active*	*Topographic reconstruction 1969–2021*	10,190 ± 3990	–	–	6.8 ± 2.7	–
	DoD 2005–2021	920 ± 365 Incised channels	1290 ± 710	–	10.7 ± 4.2	–
		3060 ± 1130 Entire slope	4750 ± 2190		11.5 ± 4.2	
P3 (western LIA moraine) *active*	*DoD 2019–2021*	6530 ± 2100	2060 ± 610	4470 ± 2180	–	–
P4 (new channels at the glacier margin) *active*	*DoD 2013–2021*	9100 ± 1180	650 ± 390	8450 ± 1245	-	62.5 ± 9.2
P5 *inactive*	*topographic reconstruction 1985–1996*	47,560 ± 2345	7600 ± 845	39,970 ± 3200	–	462.7 ± 37
P6 (Sulden I outflow) *active*	*DoD 2013–2021*	2080 ± 270	630 ± 160	1450 ± 315	–	21.1 ± 4.6
P8 (2014 landslide) *active*	*DoD 2013–2021*	11,730 ± 1270	7100 ± 1570	4630 ± 2020	–	22.8 ± 9.9

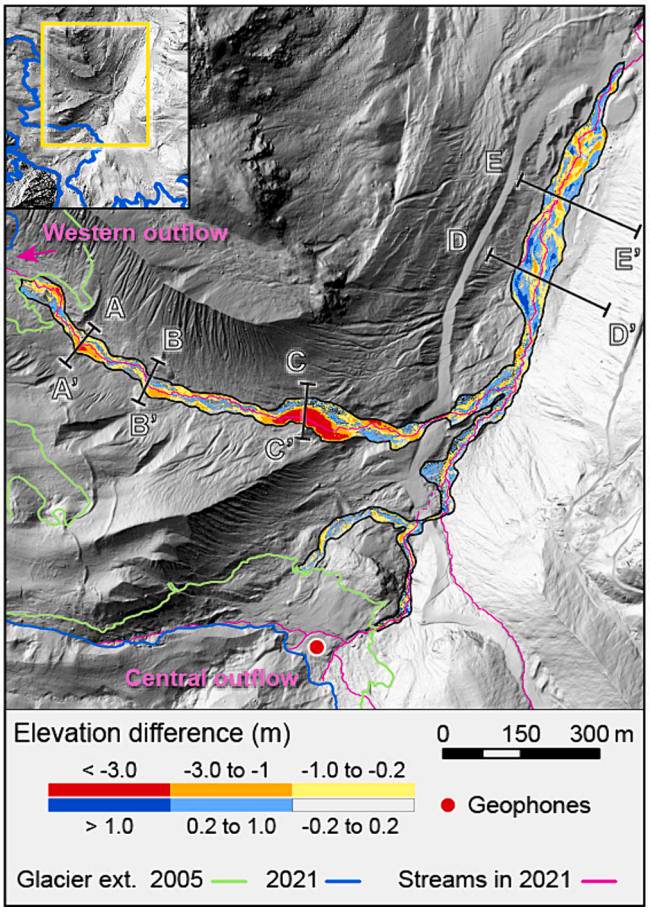

Fig. 9. Elevation difference in the analyzed proglacial channel network for the 2005–2021 period. The thin black line represents the limits of the channel system in 2021 (including lateral erosion). Cross sections (i.e., A–E) are shown in Fig. 11.

determined by the seismic survey) and from lateral fluvial erosion (i.e., through DoD analyses on the lateral portions of the proglacial streams), respectively. On average, the erosion rate equaled 16.0 mm yr^{-1} within the active channel bed, and reached 29.3 mm yr^{-1} including lateral fluvial erosion.

In the longer period of 2005–2021, the sediment mobilized within the active channel network amounted to 1500 ± 350 m^3 yr^{-1}, of which 850 ± 200 m^3 yr^{-1} (i.e., 55 %) were eroded and 700 ± 250 m^3 yr^{-1} (45 %) were deposited from the active channel bed. The net balance thus indicated a volumetric loss of 150 ± 300 m^3 yr^{-1} (only 4 %), but with a very large error that questioned its significance. The contribution of glacial and lateral fluvial erosion to the total volume of sediment transported to the outlet of the proglacial plain corresponded to 37 % (i.e., 1375 m^3 yr^{-1} from the seismic survey) and 59 % (i.e., 2200 m^3 yr^{-1} from DoD analysis on the lateral portion of the proglacial streams), respectively. On average, the erosion rate was 3.0 mm yr^{-1} within the active channel bed and reached 25.0 mm yr^{-1} when lateral fluvial erosion was considered.

4.4. Connectivity and geomorphological evolution

The analysis of the connectivity index (IC, Cavalli et al., 2013) indicated that long-term changes in the reorganization of the drainage system can effectively modify the connectivity between the contiguous landforms and their deposits of the proglacial plain (i.e., structural connectivity; Buter et al. (2022), and references therein). For example, in 2005, the presence of a western lateral stream draining the glacier margin of the main Sulden glacier allowed a large area of the glacier forefield to be connected (IC values > -1.4) to the downstream floodplain (Fig. 10). The same area was disconnected in 2021 (IC values < -4.0), when the reorganization of the drainage pattern after glacier retreat resulted in the isolation of the previously active lateral outflow (Fig. 10).

Although useful for detecting changes in structural connectivity (i.e., between contiguous landforms), the IC map derived from the 2.5 m resolution DTM failed to distinguish between areas that were connected and supplied sediment (i.e., active sediment sources) from those regions

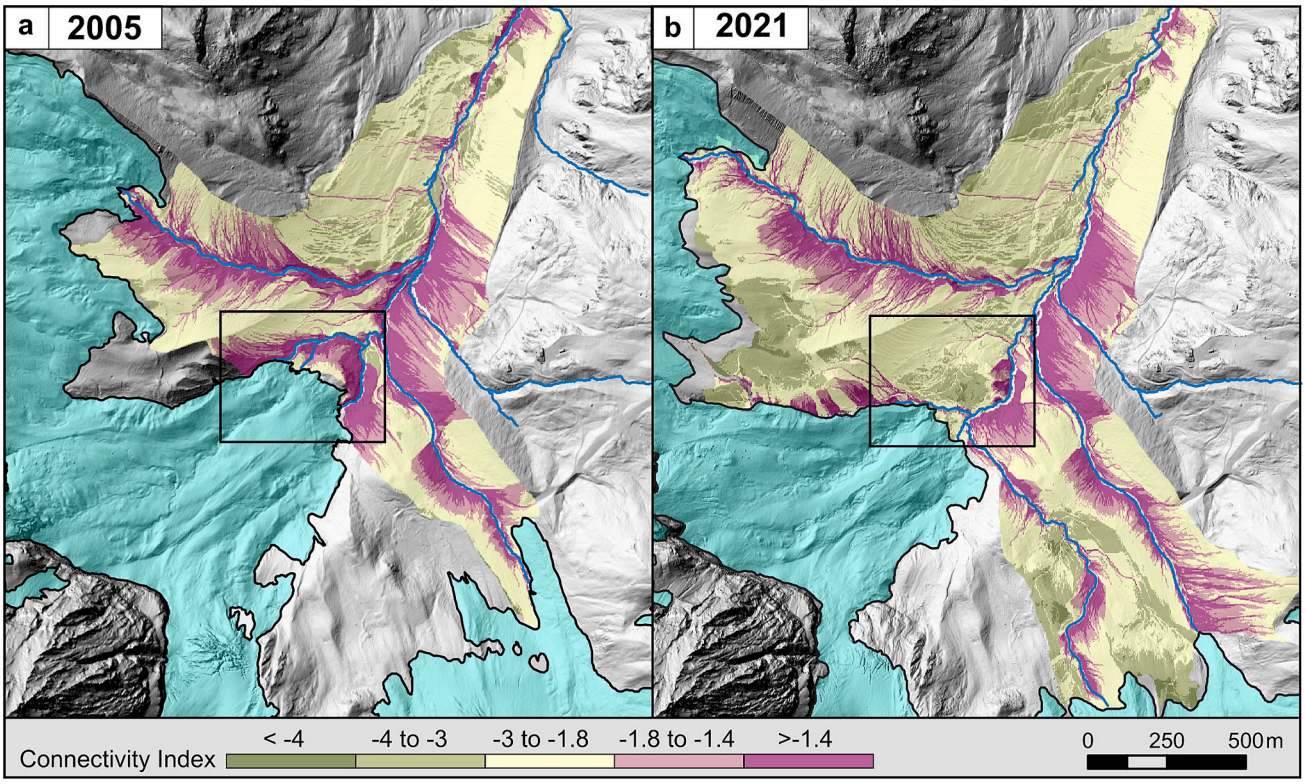

Fig. 10. IC maps for a) 2005 and b) 2021 based on 2.5 m DTM resolution. In the black rectangle, the changes in IC related to the isolation of a previously active channel.

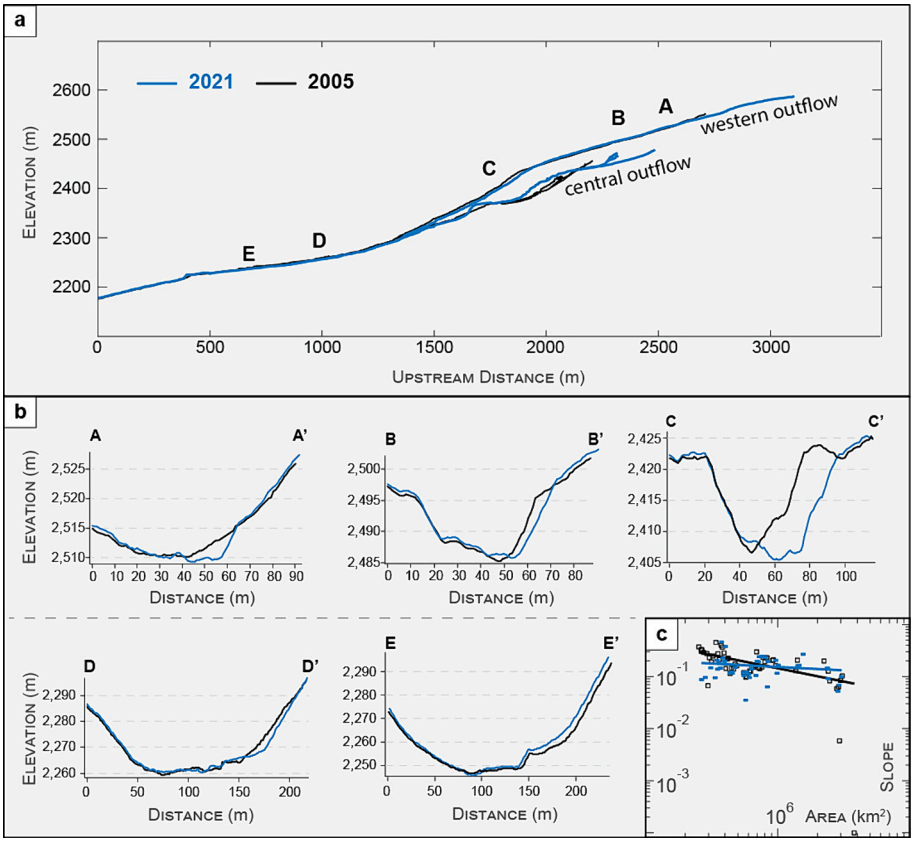

Fig. 11. a) River long profile and b) cross sections of the outflow channels; c) slope-area plot shows the tendency of the channels to be dominated by debris-flow processes (Stock and Dietrich, 2003, 2006). Profiles are shown for 2005 and 2021 to help visualize the changes that occurred during this time span.

that were connected but did not release sediment (i.e., areas that have the potential to release sediment, but do not exhibit signs of instability). This is a limitation of the technique, as the IC is solely calculated on a topographic basis and there is no previous knowledge on the location of real active sediment sources (Steger et al., 2022). Despite this, we were able to obtain a more realistic IC map by using the higher-resolution DSM (e.g., 1 m, not shown here), as even small topographic barriers prevented sediment supplied from the moraines to be connected to the proglacial stream, but the intrinsic limitation of the method remained.

Using the 2005 and 2021 DSMs, we analyzed the changes in the channel profiles of the two main outflows exiting the Sulden glacier (Fig. 11). Following the flow direction, the upper reaches show a rather straight profile, whereas the profile below an elevation of ca. 2450 m a.s.l. has a concave shape. This geometry indicates that the upper reaches are not yet in equilibrium with their runoff and sediment supply (Lane, 1955; Mackin, 1948) and are thus more easily dominated by debris-flow processes (e.g., Stock and Dietrich, 2003, 2006). The difference between the central and western outflow profiles likely reflects the type of substrate, as the central stream crosses some bedrock gorges with little sediment storage, whereas the western stream has a coarse-grained sediment bed. The cross sections in Figs. 9 and 11 confirm rather substantial lateral erosion, especially along the upper reaches of the western proglacial stream.

5. Discussion

5.1. Sediment erosion and supply from moraines and newly-formed channels

Our results confirm the extremely high dynamics of proglacial areas (Antoniazza and Lane, 2021; Carrivick and Heckmann, 2017), with very high rates of sediment erosion and remobilization through the channel network (Table 3). We observed some important differences between the processes affecting the moraines – and their evolution – and those occurring within the drainage network. In particular, most of the sediment eroded from the moraines (e.g., P1 – P3) was deposited at their toes and was thus disconnected from the proglacial streams. As observed elsewhere (e.g., Gärtner-Roer and Bast, 2019; Lane et al., 2017; Micheletti and Lane, 2016; Piermattei et al., 2023), also in the Sulden region sediment supply from moraines to channels was limited to a few locations and, based on field observations and previous work, took place mainly during rainfall events (e.g., Buter et al., 2022), or was supplied owing to lateral fluvial erosion. The most pronounced gullies were generally located in the upper and over-steepened portions of the moraine, which was less stable than previously thought (Rabanser, 2019). The presence of dead ice on the valley floor or ground ice on the moraine slopes prevented or slowed the development of the gully system, also suggested by Gärtner-Roer and Bast (2019); in such a scenario erosion propagates downslope and upstream following ice melt over a period that may have spanned from a few years (as in the case of P3) to decades (as in the case of P1). The recent increased melting of ground ice between 2019 and 2021, together with superposed intense rainfall events occurred in the analyzed years, may have been responsible for the sudden sediment release and the very rapid gully incision in P3.

In contrast, the changes observed in the Sulden proglacial channels (e.g., P4 – P6) were primarily influenced by the glacier dynamics, especially at the ice margins (e.g., Fig. 6), and had an immediate effect on the sediment entrained and transported downstream. In particular, the speed and mechanisms of glacier retreat controlled the activation or deactivation of different sediment sources (e.g., newly formed channels, as in P4) and the period of activity (varying from 1 to 10 years, following the analyses in P4 and P5). The volume of released sediment was additionally controlled by topography, and especially by the relief between the middle moraine and the channel bed. In 2021, the lower altitude of the proglacial channel compared to the middle moraine elevation may have been responsible for the reduced erosion rate observed at P4 (e.g., ca. 60 mm yr^{-1}) compared to the rate calculated for P5 (e.g., ca. 460 mm yr^{-1}), which had higher relief and thus a higher potential for erosion. These observations suggest that the proglacial channel network may provide sediments to the downstream channel sectors at very high rates, although the rapid readjustment of the channel pattern may quickly change sediment sources (e.g., deactivation of former active channels) and rates of supply.

5.2. Contributions by different geomorphic compartments

The results of our analyses indicate that a very large proportion (34–37 %) of the sediments transported through the Sulden proglacial area on a multiyear scale were derived directly from the glacier and routed through its drainage system, which is capable of transporting coarse sediments as bedload at very high rates (Arnoldi, 2022; Engel et al., 2024). Estimates were calculated based on bedload monitoring alone (see Section 3.3.) and neglect the fraction of eroded sediments moving in suspension or as very fine bedload not captured by the "Bunte" trap (grains <4 mm). However, suspended sediment typically prevails over bedload yields in glacier-fed rivers (e.g., Comiti et al., 2019; Morche et al., 2019; Mao et al., 2019; Perolo et al., 2019), and preliminary data and analyses indicate that this is true for the Sulden river as well (Bonfrisco et al., 2023).The importance of such fine sediments with regard to bulk volumes derived from DoD analysis is not known. While it may be negligible when a DoD is computed on alluvial landforms (i.e., proglacial channels and their floodplains), this may not be the case when colluvium (i.e., landslide deposits, debris flow fans) and moraines are considered in the context of volumetric differences, since substrates in these cases may be matrix-supported. Therefore, we believe that a mixed use of bedload transport data and DoD analysis for quantifying the proglacial sediment budget, as proposed in Section 4.3, is justified in terms of orders of magnitude (analogous to the analysis presented in Comiti et al., 2019). At the same time, we consider that the 34–37 % interval described in Section 4.3 for the glacial contribution to the total sediment budget should be regarded as a conservative estimate, as our analysis captured only the coarsest sediment fraction of the central snout of the glacier. This is supported by Guillon et al. (2017), for example, who showed that suspended sediment exiting the Bosson glacier (France) dominated the sediment budget of the entire proglacial area, supplying 71 % of the total volume. Similar values have been reported by Delaney et al. (2018) for the Gries glacier in Switzerland. A more accurate determination of the sediment budget would thus require detailed knowledge of the suspended sediment yield released by the glacier, as well as the spatially variable grain-size distribution of the substrates in the different landforms. This would enable a better evaluation of the sediment transport velocities and travel distances, especially for the bedload fraction (e.g., Mancini et al., 2023).

In any case, the small budget of the active channel bed, where erosion was in equilibrium with deposition, indicates that almost all of the off-channel sediment input (from the glacier and from lateral erosion) was transferred to the outlet of the proglacial area, thus indicating that the Sulden proglacial region was dominated by sediment transport within the time period analyzed (Fig. 12). This also implies that the DoD analysis computed on the active flood plain alone, does not capture the total volume of sediment mobilized and transported through the system, but rather shows only a small fraction (i.e., <5 % for the 2005–2021 time period). Within the longest period considered here (i.e., 2005–2021), the DoD analysis indicates that the proglacial reaches seem to have attained a dynamic equilibrium in which sedimentation and erosion are relatively balanced, as has been observed in other areas (e.g., Comiti et al., 2019). However, this does not imply that the proglacial plain functions only as a sedimentary conveyor belt, because transient local erosion and deposition due to fluvial processes did occur (Savi et al., 2023). Instead, these considerations indicate that sediment is moved through the proglacial plain depending on both morphology, grain sizes, and hydrology of the proglacial streams. Mancini et al.

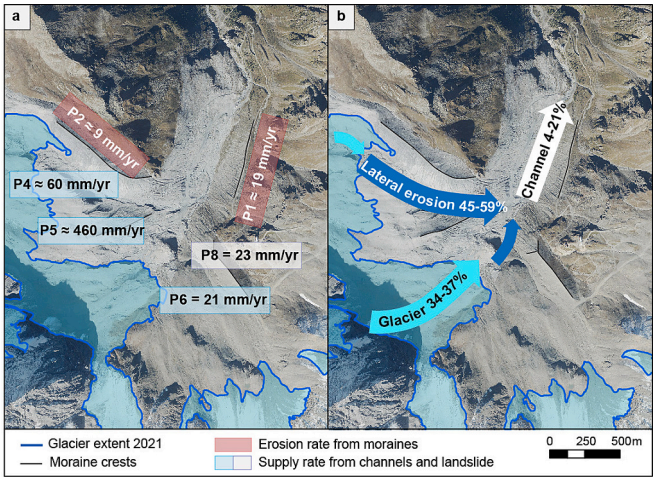

Fig. 12. a) Rates of erosion along the moraines and sediment supplied from the channel network. b) Relative contribution of glacier, lateral fluvial erosion, and in-channel erosion to the total amount of sediment exported from the proglacial plain.

(2023), for example, indicated that bedload transport through a floodplain can take up to 11 days to travel a distance of over 850 m.

5.3. Sediment budget and rates

Based on the volumetric estimates presented above and assuming a conversion factor for mass units as discussed in Section 3 as well as considering the glacial and proglacial areas as source areas, which cover a total area of 6.85 km^2, the mean annual sediment yield at the Sulden proglacial outlet is on the order of 931–1017 t yr^{-1} km^{-2}. Such values are comparable to those reported for other glaciated catchments in the Alps (Hinderer et al., 2013; Morche et al., 2019), but we caution that our data may be largely underestimated due to the missing knowledge of the glacial input from the western snout, as well as of the volumes moving in suspension.

The erosion and supply rates measured for the moraines and the proglacial plain are also consistent with those measured in other catchments with similar glaciation. For example, studies in Norway revealed that erosion rates on moraines ranged between 50 and 100 mm yr^{-1} (Ballantyne and Benn, 1994), and between 5.5 and 169 mm yr^{-1} (Curry, 1999); in Switzerland rates were calculated between 49 and 151 mm yr^{-1} (Curry et al., 2006), whereas in Austria and Italy values between 1 and 429 mm yr^{-1} (Betz-Nutz et al., 2023) and 8 and 465 mm yr^{-1} (Altmann et al., 2022) were detected. Long-term averaged erosion on the floodplain has been estimated to be approximately 4490 m^3 yr^{-1} (equal to ca. 60 mm yr^{-1} over a 28-year time period) in Switzerland (Delaney et al., 2018), and about 230 m^3 yr^{-1} for the Gepatsch Glacier in Austria (over a 66-year time period; Piermattei et al., 2023), although with important spatial and temporal variations. In our study, erosion rates between 20 and 60 mm yr^{-1} calculated for the 2005–2021 period on the moraines and along the entire channel network (i.e., including lateral fluvial erosion) are generally one order of magnitude higher than those registered in the active channel bed only (ca. 3 mm yr^{-1}). This points to reduced structural and/or functional connectivity between the basin slopes (e.g., moraines) and the channel network, as well as to the role of the proglacial plain in attenuating the downstream propagation of coarse sediments (see also e.g., Delaney et al., 2018, Antoniazza and Lane, 2021, and Mancini et al., 2023). Consequently, changes occurring in the active proglacial plain do not fully reflect the rate at which paraglacial adjustments operate in this region. Interestingly, when lateral fluvial erosion is considered, the proglacial area shows a strong erosional signal, with rates between 25 and 30 mm yr^{-1}, values that are similar to the denudation rates calculated at the end of the Younger Dryas in nearby deglaciated basins (Brardinoni et al., 2018; Savi et al., 2014).

5.4. Future scenarios and implications for sediment transport

The high lateral mobility of the Sulden outflow channels that was documented for the recent past (Figs. 9 and 11) suggests that connectivity between moraines and proglacial channels is likely to increase in the near future, thereby enhancing sediment supply to the proglacial streams through lateral erosion of the moraine toes. Nonetheless, the sediment supplied by the moraines could limit the further expansion of channel width (e.g., Malatesta et al., 2017; Tofelde et al., 2022). The effective volume of sediment supplied by the moraines is therefore difficult to predict, as moraine and channel dynamics are tightly coupled and, depending on future sediment and water discharge, may attain an autogenic equilibrium (Malatesta et al., 2017; Tofelde et al., 2022).

Although the "peak water" (i.e., the annual maximum discharge of the melting glacier; Huss and Hock, 2018) from the Sulden glacier may have already passed (Savi et al., 2021b), the prediction of the possible runoff generated by the melting glacier is subject to large uncertainties, especially in terms of timing. In fact, the Sulden glacier exhibits a complex and nonlinear behavior, with some areas melting faster than others (Savi et al., 2021b). The presence of debris on most of the glacier surface has a strong impact on melt rates (Fyffe et al., 2019) and may decouple the timing of glacier retreat from climatic forcing (Nicholson et al., 2021). Additionally, the feedbacks between melting glaciers and bedload transport are complex (e.g., Comiti et al., 2019; Coviello et al., 2022; Mao et al., 2019), and the development of a more hydraulically efficient subglacial drainage system, which might be associated with rising temperatures, for example, may enhance glacial export and transport of basal coarse-grained sediment (Fyffe et al., 2019; Perolo et al., 2019; Swift et al., 2002). However, models that have attempted to estimate future sediment supply from glaciers have provided contradictory results (Delaney and Adhikari, 2020; Raymond Pralong et al., 2015; Schmidt et al., 2024). A general, uniform temporal trajectory for glacial sediment export is likely unrealistic, because each glacier differs widely in terms of hydrology, topography, debris, and substrate (Bogen, 1996; Engel et al., 2024; Nicholson et al., 2021; Zekollari et al., 2020); for these reasons, an accurate prediction of glacier runoff and associated sediment transport would require a more profound knowledge of environmental variables that characterize subglacial conditions, but these are complex and not easy to analyze.

In the Sulden catchment, it is reasonable to assume that sediment export from the glacier may increase in the near future (e.g., until 2050), if large volumes of sediments are available at its base (e.g., Delaney et al., 2019). Unfortunately, we have no quantitative data on this. However, at the higher elevations, where the substrate below the glacier may largely constitute bedrock, we infer that ice melt may increase water discharge but not necessarily sediment input (e.g., Herman et al., 2015); if true, the transport capacity and erosional power of the subglacial streams draining the lower section of the glacier would increase. Thus, the observed proglacial dynamics can also be expected to remain relatively constant in the coming years, with high lateral mobility and limited vertical changes along the channels, as long as melt runoff, which is most effective in transporting bedload (Coviello et al., 2022), does not decline substantially in parallel with annual bedload transport capacity (Raymond Pralong et al., 2015). In the future, peaks in sediment supply associated with intense rainstorm events, "flushing" of the glacial drainage systems, lateral erosion of moraines, and proglacial channel avulsions are likely to become increasingly unbalanced by the reduced transport capacity of the proglacial streams, which are expected to undergo aggradation, and which may be further enhanced by a progressively developing vegetation cover facilitated by sandy sediments deposited on the higher fluvial surfaces (Bosson et al., 2023; Eichel et al., 2023).

5.5. Limitations and strengths of the study

At a few locations, the DoD analysis did not reliably quantify net sediment budgets due to uncertainties related to the technique used, as a threshold of 0.2 m had to be adopted for the errors inherent in the ALS surveys. This is particularly the case for volumes calculated along the moraines (e.g., at P2 and P3), where erosion in the steep and deep gullies or deposition of fine material at the foot of the moraines could easily be undetected by the analysis. In fact, these volumes were often associated with large errors or inferred sediment dynamics that contradicted the field evidence. For the P3, for example, the calculated volume of sediment entrained in the fluvial system was likely too high, since field evidence and orthophoto analysis indicated that the deposited material was decoupled from the channel network. The reason for such errors could be related to the overall lowering of the terrain due to ground-ice melting (thus an overestimation of erosion) and/or an underestimation of the deposited volume linked to the use of the threshold. In addition, the formulas applied for error propagation resulted in large errors in the net budget calculated for the entire channel network, leading to ambiguity with respect to the significance of the volumes obtained.

In the long term (i.e., in the period 2005–2021), the DoD analysis has not captured short-term erosional processes that may have occurred above the glacier margin, as shown at P3. This eroded material is temporarily disconnected from the dynamics of the proglacial plain because it is trapped on top of the ice. With further ice retreat, the sediment will eventually enter the fluvial system, but with a timing that does not correspond to its release from the moraine.

With regard to glacial sediment supply, the short monitoring period between 2019 and 2020 and the large uncertainty in the seismogenically derived bedload rates are clearly important limitations for an accurate estimate of the glacial contribution to the total amount of coarse-grained sediment of the Sulden proglacial area. While we are aware of the simplifications made in this calculation, we nevertheless believe that providing a first-order quantification of the relative contribution of glacial export to the total sediment budget of a proglacial basin represents a step forward in understanding the sediment dynamics of these regions, since this type of information has been lacking in similar studies (e.g., Knight and Harrison, 2018; Koppes et al., 2010; Piermattei et al., 2023). As this information is essential for understanding the sediment dynamics of deglaciating basins, we stress the need to collect more data to better discern the role of different landscape sectors in relation to the total amount of sediment supplied to the system.

6. Conclusions

Our study of glacial and associated sedimentary processes in the Sulden proglacial area shows that glacial sediment export and the lateral reworking of sediment by proglacial streams are the dominant sources of sediment supply to the downstream river network. Between 2005 and 2021 glacial export and fluvial erosion contributed with a minimum of 34 % and in the range of 45–59 %, respectively, to the total amount of sediment mobilized within the upper Sulden basin. Most of the sediment supplied to the channel network is transported to the proglacial outlet. Although moraines at Sulden have provided sediment for >50 years, they do not seem to contribute significantly to the material entrained in the fluvial system, because they remain largely decoupled from the proglacial stream/plain. This condition may change in future if lateral fluvial erosion continues to dominate the mechanisms of channel evolution.

We suggest that the "peak sediment" supply may still have to occur in the upper Sulden basin. Indeed, the proglacial area is widening at a fast rate, leaving a large amount of unconsolidated sediment available for transport. In the near future, glacier melt and rainfall events may increase the relative contribution of glacial and fluvial sediment supply, thereby maintaining high, or increasing the volume of sediment transported through the proglacial plain. Eventually, when the proglacial streams will decrease their discharge and transport capacity, the accumulation of sediment at the front of the melting glacier is expected to become the dominant source of sediment during high-intensity rainstorm events. Our studies furthermore emphasize that the challenges in predicting future hydrological forcing and complex relationships between sediment transport dynamics and processes of sediment generation in glacial and periglacial settings call for more integrated, comparative studies, because due to regional differences every glaciated basin will most likely respond differently to climatic change.

Funding

This research was carried out under the auspices of a research grant of the Deutsche Forschungsgemeinschaft (DFG) awarded to S. Savi ("Effects of climate warming on sediment supply and debris-flow activity in high-mountain regions," grant no. SA 3360/2-1, project no. 399435624).

CRediT authorship contribution statement

Sara Savi: Writing – review & editing, Writing – original draft, Funding acquisition, Formal analysis, Data curation, Conceptualization. **Felix Pitscheider:** Writing – review & editing, Methodology. **Michael Engel:** Writing – review & editing. **Velio Coviello:** Investigation. **Manfred R. Strecker:** Writing – review & editing. **Francesco Comiti:** Writing – review & editing, Conceptualization.

Declaration of competing interest

This paper was submitted to the Special Issue where SS is a guest-editor. However, SS had no role in the peer-review process of this manuscript. The others co-authors have nothing to declare.

Data availability

Data will be made available on request.

Acknowledgments

The first author would like to thank all the people who helped during fieldwork and in the subsequent analysis and discussion of the data. In particular, I would like to thank all the young researchers who were at the Free University of Bolzano in 2019–2023 and helped to form a dynamic and enthusiastic team of brilliant minds. The research design of this study was partly conceptualized during discussions with that group.

A special and heartfelt thanks goes to Velio Coviello, who is sadly no longer with us. His sudden passing has left an enormous empty space in research and in life. With his enthusiasm and intelligence, he made a strong contribution to this paper, and for that, we will be always grateful.

Appendix A. Supplementary data

Supplementary data to this article can be found online at https://doi.org/10.1016/j.geomorph.2024.109343.

References

3PClim. Past, Present and Perspective Climate of Tirol, Südtirol-Alto Adige and Veneto. Available at: http://www.3pclim.eu/.

Altmann, M., Pfeiffer, M., Haas, F., Rom, J., Fleischer, F., Heckmann, T., Piermattei, L., Wimmer, M., Braun, L., Stark, M., Betz-Nutz, S., Becht, M., 2023. Long-term monitoring (1953–2019) of geomorphologically active sections on LIA lateral moraines under changing meteorological conditions. EGUsphere. https://doi.org/10.5194/egusphere-2022-1512 [preprint].

Anderson, S.W., Konrad, C.P., 2019. Downstream-propagatingchannel responses to decadal-scaleclimate variability in a glaciated riverbasin. J. Geophys. Res. Earth Surf. 124, 902–919. https://doi.org/10.1029/2018JF004734.

Anderson, S.W., Shean, D., 2021. Spatial and temporal controls on proglacial erosion rates: a comparison of four basins on Mount Rainier, 1960 to 2017. Earth Surf. Proc. Land. 47, 596–617. https://doi.org/10.1002/esp.5274.
Antoniazza, G., Lane, S.N., 2021. Sediment yield over glacial cycles: a conceptual model. Prog. Phys. Geogr. Earth Environ. 45 (6), 842–865. https://doi.org/10.1177/0309133321997292.
Antoniazza, G., Nicollier, T., Boss, S., Mettra, F., Badoux, A., Schaefli, B., Rickenmann, D., Lane, S.N., 2022. Hydrological drivers of bedload transport in an Alpine Watershed. Water Resour. Res. 58 https://doi.org/10.1029/2021WR030663.
Antoniazza, G., Dietze, M., Mancini, D., Turowski, J.M., Rickenmann, D., Nicollier, T., et al., 2023. Anatomy of an Alpine bedload transport event: a watershed-scale seismic-network perspective. J. Geophys. Res. Earth 128, e2022JF007000. https://doi.org/10.1029/2022JF007000.
Arnoldi, E., 2022. Seismic Monitoring of Bedload Transport in a Proglacial Stream (Sulden/Solda River, Italian Alps). Master Thesis,. University of Innsbruck (Austria) and Free University of Bolzano (Italy).
Ballantyne, C.K., 2002. A general model of paraglacial landscape response. The Holocene 12, 371–376. https://doi.org/10.1191/0959683602hl553fa.
Ballantyne, C.K., Benn, D.I., 1994. Paraglacial slope adjustment during recent deglaciation and its implications for slope evolution in formerly glaciated environments. In: Anderson, M.G., Brooks, S. (Eds.), Advances in Hillslope Processes, vol. 2. John Wiley and Sons, Chichester, pp. 1173–1195.
Besl, P., McKay, N., 1992. A method for registration of 3D shapes. IEEE Trans. Pattern Anal. Mach. Intell. 14 (2), 239–256. https://doi.org/10.1109/34.121791.
Betz-Nutz, S., Heckmann, T., Haas, F., Becht, M., 2023. Development of the morphodynamics on Little Ice Age lateral moraines in 10 glacier forefields of the Eastern Alps since the 1950s. Earth Surf. Dynam. 11, 203–226. https://doi.org/10.5194/esurf-11-203-2023.
Beylich, A.A., Laute, K., 2015. Sediment sources, spatiotemporal variability and rates of fluvial bedload transport in glacier-connected steep mountain valleys in western Norway (Erdalen and Bødalen drainage basins). Geomorphology 228, 552–567. https://doi.org/10.1016/j.geomorph.2014.10.018.
Bogen, J., 1996. Erosion rates and sediment yields of glaciers.pdf. Ann. Glaciol. 22.
Bonfrisco, M., Coviello, V., Engel, M., Nadalet, R., Dinale, R., Comiti, F., 2023. Temporal variability of bedload vs suspended sediment load in a glacier-fed Alpine river. EGU Gen. Assem. 2023, EGU23–11308. https://doi.org/10.5194/egusphere-egu23-11308.
Borselli, L., Cassi, P., Torri, D., 2008. Prolegomena to sediment and flow connectivity in the landscape: a GIS and field numerical assessment. Catena 75, 268–277.
Bosson, J.B., Huss, M., Cauvy-Fraunié, S., Clément, J.C., Costes, G., Fischer, M., Arthaud, F., 2023. Future emergence of new ecosystems caused by glacial retreat. Nature 620 (7974), 562–569 doi:10.1038/.
Brardinoni, F., Picotti, V., Maraio, S., Bruno, P.P., Cucato, M., Morelli, C., Mair, V., 2018. Postglacial evolution of a formerly glaciated valley: reconstructing sediment supply, fan building, and confluence effects at the millennial time scale. GSA Bull. 130 (9–10), 1457–1473. https://doi.org/10.1130/B31924.1.
Buter, A., Spitzer, A., Comiti, F., Heckmann, T., 2020. Geomorphology of the Sulden River basin (Italian Alps) with a focus on sediment connectivity. J. Maps 16, 890–901. https://doi.org/10.1080/17445647.2020.1841036.
Buter, A., Heckmann, T., Filisetti, L., Savi, S., Mao, L., Gems, B., Comiti, F., 2022. Effects of catchment characteristics and hydro-meteorological scenarios on sediment connectivity in glacierised catchments. Geomorphology 402, 108128. https://doi.org/10.1016/j.geomorph.2022.108128.
Carrillo, R., Mao, L., 2020. Coupling sediment transport dynamics with sediment and discharge sources in a glacial andean basin. Water (Switzerland) 12, 1–25. https://doi.org/10.3390/w12123452.
Carrivick, J.L., Heckmann, T., 2017. Short-term geomorphological evolution of proglacial systems. Geomorphology 287, 3–28.
Cavalli, M., Trevisani, S., Comiti, F., Marchi, L., 2013. Geomorphometric assessment of spatial sediment connectivity in small Alpine catchments. Geomorphology 188, 31–41. https://doi.org/10.1016/j.geomorph.2012.05.007.
Cavalli, M., Heckmann, T., Marchi, L., 2019. Sediment connectivity in proglacial areas. In: Heckmann, T., Morche, D. (Eds.), Geomorphology of Proglacial Systems. Landform and Sediment Dynamics in Recently Deglaciated Alpine Landscapes. Springer International Publishing, pp. 271–287.
Church, M., Ryder, J.M., 1972. Paraglacial sedimentation: a consideration of fluvial processes conditioned by glaciation. Geol. Soc. Am. Bull. 83, 3059–3071.
Comiti, F., Mao, L., Penna, D., Dell'Agnese, A., Engel, M., Rathburn, S., Cavalli, M., 2019. Glacier melt runoff controls bedload transport in Alpine catchments. Earth Planet. Sci. Lett. 520, 77–86. https://doi.org/10.1016/j.epsl.2019.05.031.
Cossart, E., 2008. Landform connectivity and waves of negative feedbacks during the paraglacial period, a case study: the Tabuc subcatchment since the end of the Little Ice Age (massif des Écrins, France). Géomorphol. Relief Processus, Environ. 14 (4), 249–260.
Coviello, V., Vignoli, G., Simoni, S., Bertoldi, W., Engel, M., Buter, A., Marchetti, G., Andreoli, A., Savi, S., Comiti, F., 2022. Bedload fluxes in a glacier-fed river at multiple temporal scales. Earth Sp. Sci. Open Arch. 27.
Crespi, A., Matiu, M., Bertoldi, G., Petitta, M., Zebisch, M., 2020. High resolution daily series (1980–2018) and monthly climatologies (1981-2010) of mean temperature and precipitation for Trentino – South Tyrol (north-eastern Italian Alps). PANGAEA. https://doi.pangaea.de/10.1594/PANGAEA.924502.
Crespi, A., Matiu, M., Bertoldi, G., Petitta, M., Zebisch, M., 2021. A high resolution gridded dataset of daily temperature and precipitation records (1980–2018) for Trentino – South Tyrol (north-eastern Italian Alps). Earth Syst. Sci. Data. https://doi.org/10.1594/PANGAEA.924502.
Curry, A.M., 1999. Paraglacial modification of slope form. Earth Surf. Process. Landf. 24, 1213–1228.
Curry, A.M., Cleasby, V., Zukowskyj, P., 2006. Paraglacial response of steep, sediment-mantled slopes to post-'Little Ice Age' glacier recession in the central Swiss Alps. J. Quat. Sci. 21, 211–225 (ISSN 0267–8179.).
Delaney, I., Adhikari, S., 2020. Increased subglacial sediment discharge in a warming climate: consideration of ice dynamics, glacial erosion, and fluvial sediment transport. Geophys. Res. Lett. 47, 1–11. https://doi.org/10.1029/2019GL085672.
Delaney, I., Bauder, A., Werder, M.A., Farinotti, D., 2018. Regional and annual variability in subglacial sediment transport by water for two glaciers in the Swiss alps. Front. Earth Sci. 6, 1–17. https://doi.org/10.3389/feart.2018.00175.
Delaney, I., Werder, M.A., Farinotti, D., 2019. A numerical model for fluvial transport of subglacial sediment. Case Rep. Med. 124, 2197–2223. https://doi.org/10.1029/2019JF005004.
Delaney, I., Werder, M.A., Felix, D., Albayrak, I., Boes, R.M., Farinotti, D., 2024. Controls on sediment transport from a glacierized catchment in the Swiss Alps established through inverse modeling of geomorphic processes. Water Resour. Res. 60, e2023WR035589 https://doi.org/10.1029/2023WR035589.
Dell'Agnese, A., Mao, L., Comiti, F., 2014. Calibration of an acoustic pipe sensor through bedload traps in a glacierized basin. CATENA 121, 222–231. ISSN 0341-8162. https://doi.org/10.1016/j.catena.2014.05.021.
Draebing, D., Eichel, J., 2018. Divergence, convergence, and path dependency of paraglacial adjustment of alpine lateral moraine slopes. Land Degrad Dev. 29, 1979–1990. https://doi.org/10.1002/ldr.2983.
Eichel, J., Draebing, D., Meyer, N., 2018. From active to stable: paraglacial transition of Alpine lateral moraine slopes. Land Degrad. Dev. 29, 4158–4172. https://doi.org/10.1002/ldr.3140.
Eichel, J., Stoffel, M., Wipf, S., 2023. Go or grow? Feedbacks between moving slopes and shifting plants in high mountain environments. Prog. Phys. Geogr. 47 (6), 967–985. https://doi.org/10.1177/03091333231193844.
Engel, M., Penna, D., Bertoldi, G., Vignoli, G., Tirler, W., Comiti, F., 2018. Controls on spatial and temporal variability of streamflow and hydrochemistry in a glacierized catchment. Hydrol. Earth Syst. Sci. Discuss. 1–59 https://doi.org/10.5194/hess-2018-135.
Engel, M., Coviello, V., Buter, A., Carillo, R., Miyata, S., Marchetti, G., Andreoli, A., Savi, S., Kofler, C., Scorpio, V., Nicholson, L., Comiti, F., 2020. Sediment dynamics in glacierized catchments: a comparison study from two proglacial streams in the Sulden catchment (Eastern Italian Alps). In: EGU General Assembly 2020, Online, 4–8 May 2020, EGU2020-11199. https://doi.org/10.5194/egusphere-egu2020-11199.
Engel, M., Coviello, V., Savi, S., Buter, A., Andreoli, A., Miyata, S., Marchetti, G., Scorpio, V., Rathburn, S., Nicholson, L., Comiti, F., 2024. Meltwater driven sediment transport dynamics in two contrasting Alpine proglacial streams. J. Hydrol. 635, 131171 https://doi.org/10.1016/j.jhydrol.2024.131171.
Finsterwalder, S., Legally, S., 1913. Die Neuvermessung des Suldenferners 1906 und dessen Veränderungen in den letzten Jahrzehnten. In Zeitschrift für Gletscherkunde, für Eiszeitforschung und geschichte des Klima. Annals of glaciology, Band VII Heft 3, Brückner E., et alii, Verlag von Gebrüder Borntraeger, Berlin, 1913.
Fryirs, K., Brierley, G.J., Preston, N.J., Kasai, M., 2007. Buffers, barriers and blankets: the (dis)connectivity of catchment-scale sediment cascades. Catena 70, 49–67.
Fyffe, C.L., Brock, B.W., Kirkbride, M.P., Black, A.R., Smiraglia, C., Diolaiuti, G., 2019. The impact of supraglacial debris on proglacial runoff and water chemistry. J. Hydrol. 576, 41–57. https://doi.org/10.1016/j.jhydrol.2019.06.023.
Gärtner-Roer, I., Bast, A., 2019. (Ground) ice in the proglacial zone. In: Heckmann, T., Morche, D. (Eds.), Geomorphology of Proglacial Systems. Geography of the Physical Environment. Springer, Cham. https://doi.org/10.1007/978-3-319-94184-4_6.
Gobiet, A., Kotlarski, S., Beniston, M., Heinrich, G., Rajczak, J., Stoffel, M., 2014. 21st century climate change in the European Alps-a review. Sci. Total Environ. 493, 1138–1151. https://doi.org/10.1016/j.scitotenv.2013.07.050.
Guillon, H., Mugnier, J.L., Buoncristiani, J.F., 2017. Proglacial sediment dynamics from daily to seasonal scales in a glaciated Alpine catchment (Bossons glacier, Mont Blanc massif, France). Earth Surf. Process. Landforms 43, 1478–1495. https://doi.org/10.1002/esp.4333.
Harbor, Jon, Warburton, Jeff, 1993. Relative rates of glacial and nonglacial erosion in Alpine environments. Arct. Alp. Res. 25 (1), 1–7. https://doi.org/10.1080/00040851.1993.12002973.
Herman, F., Beyssac, O., Brughelli, M., Lane, S.N., Leprince, S., Adatte, T., et al., 2015. Erosion by an Alpine glacier. Science 350 (6257), 193–195. https://doi.org/10.1126/science.aab2386.
Hinderer, M., Kastowski, Martin, Kamelger, Achim, Bartolini, Carlo, Schlunegger, Fritz, 2013. River loads and modern denudation of the Alps — a review. Earth-Sci. Rev. 118, 11–44. ISSN 0012-8252. https://doi.org/10.1016/j.earscirev.2013.01.001.
Hock, R., Rasul, G., Adler, C., Cáceres, B., Gruber, S., Hirabayashi, Y., Jackson, M., Kääb, A., Kang, S., Kutuzov, S., Milner, Al, Molau, U., Morin, S., Orlove, B., Steltzer, H., 2019. High mountain areas. In: Pörtner, H.-O., Roberts, D.C., Masson-Delmotte, V., Zhai, P., Tignor, M., Poloczanska, E., Mintenbeck, K., Alegría, A., Nicolai, M., Okem, A., Petzold, J., Rama, B., Weyer, N.M. (Eds.), IPCC Special Report on the Ocean and Cryosphere in a Changing Climate. Cambridge University Press, Cambridge, UK and New York, NY, USA, pp. 131–202. https://doi.org/10.1017/9781009157964.004.
Huss, M., Hock, R., 2018. Global-scale hydrological response to future glacier mass loss. Nat. Clim. Chang. 8, 135–140. https://doi.org/10.1038/s41558-017-0049-x.
Huss, M., Bookhagen, B., Huggel, C., Jacobsen, D., Bradley, R.S., Clague, J.J., et al., 2017. Toward mountains without permanent snow and ice. Earth's Future 5, 418–435. https://doi.org/10.1002/2016EF000514.
ISPRA, 2012. Carta Geologica d'Italia, Foglio Bormio. SystemCart, Rome.

Knight, J., Harrison, S., 2014. Mountain glacial and paraglacial environments under global climate change: Lessons from the past and future directions. Geogr. Ann. Ser. B 96, 245–264. https://doi.org/10.1111/geoa.12051.
Knight, J., Harrison, S., 2018. Transience in cascading paraglacial systems. Land Degrad. Dev. 29, 1991–2001. https://doi.org/10.1002/ldr.2994.
Kofler, C., Mair, W., Gruber, S., Todisco, M.T., Nettleton, I., Steger, S., et al., 2021. When do rock glacier fronts collapse? Insights from two case studies in South Tyrol (Italian Alps). Earth Surf. Process. Landf. https://doi.org/10.1002/esp.5099.
Koppes, Michèle, Sylwester, Richard, Rivera, Andres, Hallet, Bernard, 2010. Variations in sediment yield over the advance and retreat of a calving glacier, Laguna San Rafael, North Patagonian Icefield. Quat. Res. 73 (1), 84–95, 2010. ISSN 0033-5894. https://doi.org/10.1016/j.yqres.2009.07.006.
Lague, Dimitri, Brodu, Nicolas, Leroux, Jérôme, 2013. Accurate 3D comparison of complex topography with terrestrial laser scanner: Application to the Rangitikei canyon (N-Z). ISPRS J. Photogramm. Remote Sens. 82, 10–26. ISSN 0924-2716. https://doi.org/10.1016/j.isprsjprs.2013.04.009.
Lane, E.W., 1955. Importance of fluvial morphology in hydraulic engineering. Proc. Am. Soc. Civ. Eng. 81, 1–17.
Lane, S.N., Westaway, R.M., Murray Hicks, D., 2003. Estimation of erosion and deposition volumes in a large, gravel-bed, braided river using synoptic remote sensing. Earth Surf. Processes Landforms J. Br. Geomorphol. Res. Group 28 (3), 249–271.
Lane, S.N., Bakker, M., Gabbud, C., Micheletti, N., Saugy, J.N., 2017. Sediment export, transient landscape response and catchment-scale connectivity following rapid climate warming and Alpine glacier recession. Geomorphology 277, 210–227. https://doi.org/10.1016/j.geomorph.2016.02.015.
Mackin, J.H., 1948. Concept of the graded river. Bull. Geol. Soc. Am. 69, 463–512.
Malatesta, L.C., Prancevic, J.P., Avouac, J.P., 2017. Autogenic entrenchment patterns and terraces due to coupling with lateral erosion in incising alluvial channels. J. Geophys. Res. Earth 122, 335–355. https://doi.org/10.1002/2015JF003797.
Mancini, D., Lane, S.N., 2020. Changes in sediment connectivity following glacial debuttressing in an Alpine valley system. Geomorphology 352, 106987. https://doi.org/10.1016/j.geomorph.2019.106987.
Mancini, D., Dietze, M., Müller, T., Jenkin, M., Miesen, F., Roncoroni, M., et al., 2023. Filtering of the signal of sediment export from a glacier by its proglacial forefield. Geophys. Res. Lett. 50, e2023GL106082 https://doi.org/10.1029/2023GL106082.
Mao, L., Dell'Agnese, A., Huincache, C., Penna, D., Engel, M., Niedrist, G., Comiti, F., 2014. Bedload hysteresis in a glacier-fed mountain river. Earth Surf. Process. Landforms 39, 964–976. https://doi.org/10.1002/esp.3563.
Mao, L., Comiti, F., Carrillo, R., Penna, D., 2019. In: Heckmann, T., Morche, D. (Eds.), Sediment Transport in Proglacial Rivers, pp. 199–217. https://doi.org/10.1007/978-3-319-94184-4_12.
McColl, S.T., Draebing, D., 2019. Rock slope instability in the proglacial zone: state of the art. In: Heckmann, T., Morche, D. (Eds.), Geomorphology of Proglacial Systems, Geography of the Physical Environment. Springer Nature Switzerland AG 2019. https://doi.org/10.1007/978-3-319-94184-4_8.
Micheletti, N., Lane, S.N., 2016. Water yield and sediment export in small, partially glaciated Alpine watersheds in a warming climate. Water Resour. Res. 52, 4924–4943. https://doi.org/10.1002/2016WR018774.
Morche, D., Baewert, H., Schuchardt, A., Faust, M., Weber, M., Khan, T., 2019. Fluvial sediment transport in the proglacial Fagge River, Kaunertal, Austria. In: Heckmann, T., Morche, D. (Eds.), Geomorphology of Proglacial Systems. Geography of the Physical Environment. Springer, Cham. https://doi.org/10.1007/978-3-319-94184-4_13.
Nicholson, L., Wirbel, A., Mayer, C., Lambrecht, A., 2021. The challenge of non-stationary feedbacks in modeling the response of debris-covered glaciers to climate forcing. Front. Earth Sci. 9, 1–18. https://doi.org/10.3389/feart.2021.662695.
Nourbakhshbeidokhti, S., Kinoshita, A.M., Chin, A., Florsheim, J.L.A., 2019. Workflow to estimate topographic and volumetric changes and errors in channel sedimentation after disturbance. Remote Sens. (Basel) 11 (5), 586. https://doi.org/10.3390/rs11050586.
Perolo, P., Bakker, M., Gabbud, C., Moradi, G., Rennie, C., Lane, S.N., 2019. Subglacial sediment production and snout marginal ice uplift during the late ablation season of a temperate valley glacier. Earth Surf. Process. Landforms 44, 1117–1136. https://doi.org/10.1002/esp.4562.
Piermattei, L., Heckmann, T., Betz-Nutz, S., Altmann, M., Rom, J., Fleischer, F., Stark, M., Haas, F., Ressl, C., Wimmer, M.H., Pfeifer, N., Becht, M., 2023. Evolution of an Alpine proglacial river during 7 decades of deglaciation. Earth Surf. Dynam. 11, 383–403. https://doi.org/10.5194/esurf-11-383-2023.
Porter, P.R., Smart, M., Irvine-Fynn, T., 2019. Glacial sediment stores and their reworking. In: Heckmann, T., Morche, D. (Eds.), Geomorphology of Proglacial Systems: Landform and Sediment Dynamics in Recently Deglaciated Alpine Landscapes. (Geography of the Physical Environment). Springer Nature, pp. 157–176. https://doi.org/10.1007/978-3-319-94184-4_10.
Rabanser, M., 2019. Processes of Lateral Moraine Formation at a Debris - Covered Glacier, Suldenferner (Vedretta di Solda), Master thesis at Lund University, 2019.
Raymond Pralong, M., Turowski, J.M., Rickenmann, D., Zappa, M., 2015. Climate change impacts on bedload transport in alpine drainage basins with hydropower exploitation. Earth Surf. Process. Landforms 40, 1587–1599. https://doi.org/10.1002/esp.3737.
Rickenmann, D., 2018. Variability of bed load transport during six summers of continuous measurements in two Austrian mountain streams (Fischbach and Ruetz). Water Resour. Res. 54 (1), 107–131. https://doi.org/10.1002/2017WR021376.
Savi, S., Norton, K., Picotti, V., Akçar, N., Delunel, R., Brardinoni, F., Kubik, P.W., Schlunegger, F., 2014. Quantifying sediment supply at the end of the last glaciation: dynamic reconstruction of an alpine debris-flow fan. Geol. Soc. Am. Bull. 126 (5–6), 773–790. https://doi.org/10.1130/B30849.1.
Savi, S., Comiti, F., Strecker, M.R., 2021a. Pronounced increase in slope instability linked to global warming: a case study from the eastern European Alps. Earth Surf. Process. Landforms 46, 1328–1347. https://doi.org/10.1002/esp.5100.
Savi, S., Dinale, R., Comiti, F., 2021b. The sulden/solda glacier (Eastern Italian Alps): fluctuations, dynamics, and topographic control over the last 200 years. Geogr. Fis. Dinam. Quat. 44, 15–30. https://doi.org/10.4461/GFDQ.2021.44.2.
Savi, S., Buter, A., Heckmann, T., Theule, J., Mao, L., Comiti, F., 2023. Multi-temporal analysis of morphological changes in an Alpine proglacial area and their effect on sediment transfer. Catena 220, 106701. https://doi.org/10.1016/j.catena.2022.106701.
Schmidt, L.K., Francke, T., Rottler, E., Blume, T., Schöber, J., Bronstert, A., 2022. Suspended sediment and discharge dynamics in a glaciated alpine environment: identifying crucial areas and time periods on several spatial and temporal scales in the Ötztal, Austria. Earth Surf. Dynam. 10, 653–669. https://doi.org/10.5194/esurf-10-653-2022.
Schmidt, L.K., Francke, T., Grosse, P.M., Bronstert, A., 2024. Projecting sediment export from two highly glacierized alpine catchments under climate change: exploring non-parametric regression as an analysis tool. Hydrol. Earth Syst. Sci. 28, 139–161. https://doi.org/10.5194/hess-28-139-2024.
Scorpio, V., Cavalli, M., Steger, S., Crema, S., Marra, F., Zaramella, M., Borga, M., Marchi, L., Comiti, F., 2022. Storm characteristics dictate sediment dynamics and geomorphic changes in mountain channels: a case study in the Italian Alps. Geomorphology 403, 108173. https://doi.org/10.1016/j.geomorph.2022.108173.
Slaymaker, O., 2009. Proglacial, periglacial or paraglacial? In: Knight, J., Harrison, S. (Eds.), Periglacial and Paraglacial Processes and Environments. The Geological Society Publishing House, London, pp. 71–84.
Steger, S., Scorpio, V., Comiti, F., Cavalli, S., 2022. Data-driven modelling of joint debris flow release susceptibility and connectivity. Earth Surf. Process. Landf. https://doi.org/10.1002/esp.5421.
Stock, J., Dietrich, W.E., 2003. Valley incision by debris flows: evidence of a topographic signature. Water Resour. Res. 39 (4), 1089. https://doi.org/10.1029/2001WR001057.
Stock, J., Dietrich, W.E., 2006. Erosion of steepland valleys by debris flows. GSA Bullettin 118 (9/10), 1125–1148. https://doi.org/10.1130/B25902.1.
Swift, D.A., Nienow, P.W., Spedding, N., Hoey, T.B., 2002. Geomorphic implications of subglacial drainage configuration: rates of basal sediment evacuation controlled by seasonal drainage system evolution. Sediment. Geol. 149, 5–19. https://doi.org/10.1016/S0037-0738(01)00241-X.
Szypuła, Bartłomiej, 2019. Quality assessment of DEM derived from topographic maps for geomorphometric purposes. Open Geosci. 11, 843–865. https://doi.org/10.1515/geo-2019-0066.
Taylor, J., 1997. An Introduction to Error Analysis: The Study of Uncertainties in Physical Measurements, 2nd edn. Sausalito, CA, University Science Books.
Tofelde, S., Bufe, A., Turowski, J.M., 2022. Hillslope sediment supply limits alluvial valley width. AGU Adv. 3, e2021AV000641 https://doi.org/10.1029/2021AV000641.
Von Sonklar, K., 1857. Der neuerliche Ausbruch des Suldnergletschers in Tirol. Academie der Wissenschaften, Wien, 1857.
Wheaton, J.M., Brasington, J., Darby, S.E., Sear, D.A., 2010. Accounting for uncertainty in DEMs from repeat topographic surveys: improved sediment budgets. Earth Surf Process Land 35, 136–156. https://doi.org/10.1002/esp.1886.
Zekollari, H., Huss, M., Farinotti, D., 2020. On the imbalance and response time of glaciers in the European Alps. Geophys. Res. Lett. 47, 1–9. https://doi.org/10.1029/2019GL085578.
Zhang, T., Li, D., East, A.E., et al., 2022. Warming-driven erosion and sediment transport in cold regions. Nat. Rev. Earth Environ. 3, 832–851. https://doi.org/10.1038/s43017-022-00362-0.